Electronic Supplementary Material (ESI) for ChemComm.

<Supplementary information>

A cyclic manipulation of cage isomers via anion exchange and unique isomerism

Seonghyeon Park,[1] Dongwon Kim,[1] Doheon Kim,[1] Dongwook Kim[2] and Ok-Sang Jung[1,*]

[1] Department of Chemistry, Pusan National University, Busan 46241, Republic of Korea
[2] Center for Hydrocarbon Functionalizations, IBS, Daejon 34141, Republic of Korea
Fax: (+82) 51-5163522; Tel: (+82) 51-5103240; E-mail: oksjung@pusan.ac.kr

Experimental Procedures

Materials and Physicochemical Measurements.
All chemicals including palladium(II) nitrate were purchased from Sigma-Aldrich and used without further purification. PdX_2 (X^- = BF_4^- and ClO_4^-) was prepared by anion exchange of $PdCl_2$ with AgX. Elemental microanalyses (C, H, N) were performed on crystalline samples at the KBSI Busan Center using a Vario-EL III analyzer. Infrared spectra were obtained on a Nicolet 380 FT-IR spectrophotometer using samples prepared as KBr pellets. ^1H and ^{13}C NMR spectra were recorded on a Varian Mercury Plus 300 or an Agilent Superconducting FT-NMR 600 MHz Spectrometer, ^{11}B and ^{19}F NMR spectra on an Agilent Superconducting FT-NMR 600 MHz Spectrometer while the ^{11}B and ^{19}F chemical shifts were automatically determined. Thermal analyses were performed under N_2 at a scan rate of 10 °C/min using a Perkin Elmer-TGA-DSC 4000. Electrospray time of flight ionization mass spectrometry (ESI-TOF-MS) was recorded on a Synapt G2 mass spectrometer (WATERS) at Ochang center, KBSI.

Synthesis of Cyclohexyl(methyl)bis(3-pyridyl)silane (L).
To a solution of 3-bromopyridine (6.32 g, 40 mmol) in dry diethyl ether (70 mL) under a nitrogen gas atmosphere, n-butyllithium (18 mL of 2.5 M solution in n-hexane, 45 mmol) was added dropwise at -78 °C. The resulting mixture was allowed to warm to 0 °C, after which it was stirred for 1 h. Then, (cyclohexyl)(methyl)dichlorosilane (3.61 mL, 20 mmol) was slowly added to the yellow suspension at -78 °C, and then the reaction mixture was stirred at room temperature for 12 h. Distilled water (40 mL) subsequently was added, and the organic layer was separated. The organic solution was washed with distilled water several times, and then was dried over anhydrous magnesium sulfate. The crude product was then purified by column chromatography using ethyl acetate and n-hexane as eluents. The solvent was evaporated to obtain a yellowish-brown viscous liquid in a 70.0% yield (3.95 g). Anal. Calcd for C, 72.29; H, 7.85; N, 9.92%. Found: C, 71.60; H, 7.71; N, 9.78. ^1H NMR (300 MHz, Me_2SO-d_6, δ): 8.65 (s, 2H), 8.59 (d, J = 4.70 Hz, 2H), 7.88 (d, J = 7.63 Hz, 2H), 7.39 (t, J = 12.33 Hz, 2H), 1.68-1.10 (m, 11H), 0.59 (s, 3H). IR (KBr pellet, cm-1): 1577 (m), 1573 (s), 1565 (m), 1473 (w), 1446 (w), 1400 (m), 1396 (s), 1330 (m), 1253 (m), 1222 (w), 1195 (m), 1122 (m), 1029 (m), 887 (m), 783 (s), 713 (s), 474 (m).

***endo*-Me_8-$[(NO_3)_2@Pd_4L_8](NO_3)_6 \cdot 5Me_2SO$ (via Self-Assembly).**
The reaction of $Pd(NO_3)_2$ (0.1 mmol, 23 mg) with L (0.2 mmol, 56 mg) in Me_2SO at 70 °C was stirred for 12 h. Then, ethyl acetate was slowly diffused into the solution, which resulted in colorless crystals after 7 days in a 67% yield. m.p. 258 °C (dec). Anal. Calcd for C, 51.61; H, 5.71; N, 10.47. Found: C, 50.90; H, 5.66; N, 10.40. ^1H NMR (300 MHz, Me_2SO-d_6, δ): 9.68 (s, 1H), 9.60 (s, 1H), 9.36 (d, J = 4.70 Hz, 1H), 9.29 (d, J = 5.28 Hz, 1H), 8.60 (d, J = 7.04 Hz, 1H), 8.22 (d, J = 6.46 Hz, 1H), 7.71 (t, J = 12.33 Hz, 2H), 1.77-1.15 (m, 11H), 0.93 (s, 3H). IR (KBr pellet, cm^{-1}): 1591 (m), 1483 (w), 1384 (s, NO_3^-), 1263 (w), 1197 (w), 1124 (w), 1029 (w), 956 (w), 887 (w), 792 (m), 703 (m), 532 (w), 499 (w).

***exo*-Me$_4$,*endo*-Me$_4$-[(NO$_3$)$_2$@Pd$_4$L$_8$](NO$_3$)$_6$·5Me$_2$SO (via Anion Exchange).**
An aqueous solution of $NaNO_3$ (42.0 mg, 0.5 mmol) was added to a suspension of microcrystalline *exo*-Me$_4$,*endo*-Me$_4$-[(ClO$_4$)$_2$@Pd$_4$L$_8$](ClO$_4$)$_6$·5Me$_2$SO (19.4 mg, 0.005 mmol; synthesized as described below) in water (8 mL) at room temperature. The reaction mixture was stirred for 5 days, filtered, and washed with several aliquots of water and ethyl acetate. The exchanged product was recrystallized in a mixture of Me_2SO and ethyl acetate for 7 days to obtain single crystals in a 59% yield. m.p. 265 °C. Anal. Calcd for C, 51.34; H, 5.58; N, 10.57. Found: C, 50.90; H, 5.64; N, 10.51. ^{1}H NMR (300 MHz, Me_2SO-d_6, δ): 8.86 (t, J = 11.74 Hz, 1H), 8.72-8.58 (m, 3H), 8.51-8.43 (m, 3H), 8.36 (s, 2H), 8.07 (t, J = 14.67 Hz, 1H), 8.00 (d, J = 5.87 Hz, 1H), 7.96 (d, J = 4.70 Hz, 1H), 7.86 (t, J = 11.74 Hz, 11H), 7.66 (t, J = 12.91 Hz, 3H), 7.47 (q, J = 19.96 Hz, 1H), 7.36 (t, J = 8.80 Hz, 1H), 7.11-7.04 (m, 1H), 1.60-0.09 (m, 11H), 0.69 (s, 3H), 0.59 (s, 3H). IR (KBr pellet, cm^{-1}): 1591 (m), 1483 (w), 1384 (s, NO_3^-), 1344 (w), 1207 (w), 1135 (w), 1083 (w), 956 (w), 887 (w), 844 (w), 819 (w), 790 (m), 757 (w), 700 (w), 422 (w).

***exo*-Me$_4$,*endo*-Me$_4$-[(BF$_4$)$_2$@Pd$_4$L$_8$](BF$_4$)$_6$·4Me$_2$SO (via Self-Assembly).**
The self-assembly reaction of $Pd(BF_4)_2$ (0.1 mmol, 28 mg) with L (0.2 mmol, 56 mg) in Me_2SO at 70 °C for 12 h gave rise to the crude product. Ethyl acetate was slowly diffused to the reaction solution to obtain single crystals after 10 days in a 59% yield. m.p. 267 °C (dec). Anal. Calcd for C, 48.33; H, 5.25; N, 6.63. Found: C, 48.10; H, 5.34; N, 6.50. ^{1}H NMR (600 MHz, Me_2SO-d_6, δ): 8.74 (d, J = 5.65 Hz, 1H), 8.53 (d, J = 5.65 Hz, 1H), 8.50 (s, 1H), 8.39 (d, J = 9.00 Hz, 2H), 8.34 (d, J = 7.48 Hz, 1H), 8.29(s, 1H), 7.96 (d, J = 7.48 Hz, 1H), 7.92 (d, J = 5.49 Hz, 1H), 7.89 (d, J = 5.34 Hz, 1H), 7.76 (t, J = 13.12 Hz, 1H), 7.55 (t, J = 13.28 Hz, 1H), 7.47 (br, 1H), 7.37 (t, J = 13.43 Hz, 1H), 7.26 (t, J = 13.28 Hz, 1H), 6.97 (d, J = 7.48 Hz, 1H), 1.55-0.00 (m, 22H), 0.53 (d, J = 28.99 Hz, 6H). ^{13}C NMR (Me_2SO-d_6, δ): 157.08, 156.90, 156.47, 154.54, 153.57, 152.22, 148.15, 147.44, 146.69, 135.22, 134.60, 133.78, 131.07, 127.83, 127.24, 126.76, 28.95-20.99, -8.20, 9.08. IR (KBr pellet, cm^{-1}): 1643 (br, m), 1593 (s), 1479 (w), 1444 (w), 1406 (m), 1342 (m), 1263 (w), 1203 (w), 1035 (br, BF_4^-), 953 (w), 887 (w), 793 (s), 761 (m), 700 (m), 522 (w), 457 (w).

***endo*-Me$_8$-[(BF$_4$)$_2$@Pd$_4$L$_8$](BF$_4$)$_8$·5Me$_2$SO (via Anion Exchange).**
An aqueous solution of NH_4BF_4 (52.4 mg, 0.5 mmol) was added to a suspension of microcrystalline *endo*-Me$_8$-[(NO$_3$)$_2$@Pd$_4$L$_8$](NO$_3$)$_6$·5Me$_2$SO (17.9 mg, 0.005 mmol) in water (8 mL) at room temperature. The reaction mixture was stirred for 24 h, filtered, and washed with several aliquots of water and ethyl acetate. Recrystallization in a mixture of Me_2SO and ethyl acetate resulted in the formation of crystals after 7 days in a 60% yield. m.p. 266 °C (dec). Anal. Calcd for C, 46.51; H, 5.51; N, 5.94. Found: C, 46.70; H, 5.60; N, 5.80. ^{1}H NMR (600 MHz, Me_2SO-d_6, δ): 9.67 (d, J = 7.78 Hz, 1H), 9.61 (d, J = 10.07 Hz, 1H), 9.48 (s, 1H), 9.37 (d, J = 5.65 Hz, 1H), 9.34 (t, J = 15.11 Hz, 2H), 9.28 (t, J = 11.60 Hz, 2H), 8.59 (d, J = 5.49 Hz, 2H), 8.21 (d, J = 5.19 Hz, 2H), 7.72 (q, J = 16.63 Hz, 4H), 1.91-0.50 (m, 22H), 0.94 (d, J = 10.83 Hz, 3H), 0.80 (d, J = 12.82 Hz, 3H). IR (KBr pellet, cm^{-1}): 1592 (m), 1477 (w), 1446 (w), 1408 (m), 1342 (w), 1261 (w), 1203 (w), 1083 (br, BF_4^-), 953 (w), 887 (w), 793 (s), 705 (m), 605 (w), 566 (w), 532 (m), 499 (w), 460 (w), 432 (w).

***exo*-Me_4,*endo*-Me_4-$[(ClO_4)_2@Pd_4L_8](ClO_4)_6 \cdot 5Me_2SO$ (via Self-Assembly).**
The reaction of $PdCl_2$ (0.1 mmol, 18 mg) with $AgClO_4$ (0.2 mmol, 41 mg) in Me_2SO at 50 °C for 1h produced $Pd(ClO_4)_2$. Then, self-assembly of $Pd(ClO_4)_2$ (0.1 mmol, 31 mg) with L (0.2 mmol, 56 mg) in Me_2SO at 70 °C for 12 h was accomplished. Ethyl acetate was slowly diffused into the reaction solution to obtain colorless crystals after 10 days in 62% yields. m.p. 319 °C (dec). Anal. Calcd for C, 46.93; H, 5.10; N, 6.44. Found: C, 46.30; H, 5.21; N, 6.30. ^{1}H NMR (600 MHz, Me_2SO-d_6, δ): 8.81 (d, J = 5.87 Hz, 1H), 8.59 (s, 1H), 8.58 (s, 1H), 8.46 (s, 1H), 8.43 (d, J = 4.70 Hz, 2H), 8.39 (d, J = 7.63 Hz, 1H), 8.32 (s, 1H), 8.01 (d, J = 7.63 Hz 1H), 7.95 (d, J = 5.87 Hz, 1H), 7.91 (d, J = 5.28 Hz, 1H), 7.82 (t, J = 12.91 Hz, 1H), 7.61 (t, J = 13.50 Hz 1H), 7.42 (t, J = 13.50 Hz, 1H), 7.32 (t, J = 13.50 Hz, 1H), 7.04 (d, J = 7.63 Hz, 1H), 1.62-0.08 (m, 22H), 0.65 (s, 1H), 0.55 (s, 1H). IR (KBr pellet, cm^{-1}): 1592 (m), 1477 (w), 1466 (w), 1404 (m), 1338 (m), 1265 (w), 1207 (w), 1087 (br, ClO_4^-), 1025 (w), 790 (s), 698 (s), 625 (s), 524 (w), 455 (m).

***endo*-Me_8-$[(ClO_4)_2@Pd_4L_8](ClO_4)_6 \cdot 5Me_2SO$ (via Anion Exchange).**
An aqueous solution of NH_4ClO_4 (52.4 mg, 0.5 mmol) was added to a suspension of microcrystalline *endo*-Me_8-$[(NO_3)_2@Pd_4L_8](NO_3)_6 \cdot 5Me_2SO$ (17.9 mg, 0.005 mmol) in water (8 mL) at room temperature. The reaction mixture was stirred for 24 h, filtered, and washed with several aliquots of water and ethyl acetate. Recrystallization in a mixture of Me_2SO and ethyl acetate resulted in the formation of crystals after 7 days in a 70% yield. m.p. 266 °C (dec). Anal. Calcd for C, 46.23; H, 5.21; N, 6.16. Found: C, 46.20; H, 5.34; N, 6,20. ^{1}H NMR (600 MHz, Me_2SO-d_6, δ): 9.63 (t, J = 30.52 Hz 1H), 9.61 (t, J = 31.69 Hz, 1H), 9.45 (s, 1H), 9.43 (s, 1H), 9.35 (d, J = 5.28 Hz, 1H), 9.32 (t, J = 11.15 Hz, 2H), 9.26 (d, J = 5.84 Hz, 1H), 8.56 (d, J = 7.63 Hz, 2H), 8.19 (d, J = 8.22 Hz, 2H), 7.71 (t, J = 12.91 Hz, 2H), 7.68 (t, J = 12.91 Hz, 2H), 1.75-0.75 (m, 22H), 0.79 (s, 3H), 0.75 (s, 3H). IR (KBr pellet, cm^{-1}): 1592 (m), 1481 (w), 1446 (w), 1407 (m), 1342 (m), 1261 (w), 1203 (w), 1087 (br, ClO_4^-), 1026 (m), 952 (w), 887 (w), 794 (s), 705 (m), 624 (s), 524 (m), 450 (m), 416 (w)

***endo*-Me_8-$[(NO_3)_2@Pd_4L_8](PF_6)_6 \cdot 4Me_2SO$ (via Anion Exchange).**
An aqueous solution of $NaPF_6$ (83.9 mg, 0.5 mmol) was added to a suspension of microcrystalline *endo*-Me_8-$[(NO_3)_2@Pd_4L_8](NO_3)_6 \cdot 5Me_2SO$ (17.9 mg, 0.005 mmol) in water (8 mL) at room temperature. The reaction mixture was stirred for 24 h, filtered, and washed with several aliquots of water and ethyl acetate. The exchanged product was recrystallized in a mixture of Me_2SO and ethyl acetate for 7 days to obtain single crystals in a high, 62% yield. Anal. Calcd for C, 53.83; H, 6.27; N, 7.85. Found: C, 53.60; H, 6.64; N, 7.74. ^{1}H NMR (300 MHz, Me_2SO-d_6, δ): 9.68 (s, 1H), 9.60 (s, 1H), 9.36 (d, J = 4.70 Hz 1H), 9.29 (d, J = 5.28 Hz 1H), 8.60 (d, J = 7.04 Hz, 1H), 8.22(d, J = 6.46 Hz, 1H), 7.71 (t, J = 12.33 Hz, 2H), 1.77-1.15 (m, 11H), 0.93 (s, 3H). IR (KBr pellet, cm^{-1}): 1592 (m), 1446 (w), 1384 (s, NO_3^-), 1345 (m), 1265 (w), 1029 (w), 845 (s, PF_6^-), 790 (m), 705 (w), 667 (w), 559 (m), 463 (br).

***endo*-Me_8-$[(NO_3)_2@Pd_4L_8](CF_3SO_3)_6 \cdot 2Me_2SO$ (via Anion Exchange).**

An aqueous solution of $NaCF_3SO_3$ (86.0 mg, 0.5 mmol) was added to a suspension of microcrystalline *endo*-Me_8-[$(NO_3)_2$@Pd_4L_8]$(NO_3)_6$·5Me_2SO (17.9 mg, 0.005 mmol) in water (8 mL) at room temperature. The reaction mixture was stirred for 24 h, filtered, and washed with several aliquots of water and ethyl acetate. The exchanged species was recrystallized in a mixture of Me_2SO and ethyl acetate, affording single crystals after 7 days in a 70% yield. Anal. Calcd for C, 46.05; H, 4.79; N, 6.81. Found: C, 46.50; H, 4.71; N, 6.74. ^{1}H NMR (300 MHz, Me_2SO-d_6, δ): 9.68 (s, 1H), 9.60 (s, 1H), 9.36 (d, J = 4.70 Hz, 1H), 9.29 (d, J = 5.28 Hz, 1H), 8.60 (d, J = 7.04 Hz, 1H), 8.22(d, J = 6.46 Hz, 1H), 7.71 (t, J = 12.33 Hz, 2H), 1.77-1.15 (m, 11H), 0.93 (s, 3H). IR (KBr pellet, cm^{-1}): 1592 (m), 1384 (s, NO_3^-), 1257 (br, $CF_3SO_3^-$), 1226 (w), 1161 (m, $CF_3SO_3^-$), 1029 (s), 887 (w), 790 (m), 706 (w), 640 (m), 451 (br).

X-ray Single Crystallography.

All of the diffraction data were measured at 100 K, respectively, with synchrotron radiation (λ = 0.6500 - 0.8000 Å, respectively) on a Rayonix MX225HS detector at 2D SMC with a silicon (111) double-crystal monochromator (DCM) at the Pohang Accelerator Laboratory (PAL), Korea. The PAL BL2D-SMDC program[1] was used for data collection (detector distance: 66 mm, omega scan Δω = 1°, exposure time: 1 s per frame), and HKL3000sm (ver. 703r)[2] was employed for cell refinement, reduction, and absorption correction. The structures were solved by the direct method and refined by full-matrix least squares techniques (SHELXL 2018/03).[3] The non-hydrogen atoms were refined anisotropically, and the hydrogen atoms were placed in calculated positions and refined using a riding model. The crystal parameters and procedural information corresponding to the data collection and structural refinement are listed in Table S2.

Cages	Pd···Pd Distances (Å)	Py···Si···Py Angles (°)
exo-Me_4,*endo*-Me_4-[$(NO_3)_2$@Pd_4L_8]$(NO_3)_6$·5Me_2SO	7.361(2) x 8.935(3)	102.5(6) ~ 113.3(7)
endo-Me_8-[$(NO_3)_2$@Pd_4L_8]$(NO_3)_6$·5Me_2SO	8.082(1) x 9.339(1)	104.7(5) ~ 108.1(7)
exo-Me_4,*endo*-Me_4-[$(BF_4)_2$@Pd_4L_8]$(BF_4)_6$·4Me_2SO	7.303(2) x 8.913(3)	103.9(4) ~ 110.7(3)
endo-Me_8-[$(BF_4)_2$@Pd_4L_8]$(BF_4)_8$·5Me_2SO	7.851(2) x 9.394(5)	106.4(3) ~ 107.5(2)
exo-Me_4,*endo*-Me_4-[$(ClO_4)_2$@Pd_4L_8]$(ClO_4)_6$·5Me_2SO	7.256(2) x 8.966(2)	104.6(5) ~ 109.9(6)
endo-Me_8-[$(ClO_4)_2$@Pd_4L_8]$(ClO_4)_6$·5Me_2SO	7.812(2) x 9.398(5)	106.4(2) ~ 107.7(2)
endo-Me_8-[$(NO_3)_2$@Pd_4L_8]$(PF_6)_6$·4Me_2SO	7.894(2) x 9.280(2)	104.8(2) ~ 107.5(2)
endo-Me_8-[$(NO_3)_2$@Pd_4L_8]$(CF_3SO_3)_6$·2Me_2SO	7.980(2) x 9.490(4)	106.0(2) ~ 108.0(2)

Table S1. Relevant Crystallographic Distances and Angles.

Table S2. Crystal Data and Refinement Parameters for (a) *endo*-Me_8-$[(NO_3)_2@Pd_4L_8](NO_3)_6$·$5Me_2SO$, (b) *exo*-$Me_4$-*endo*-$Me_4$-$[(NO_3)_2@Pd_4L_8](NO_3)_6$·$4Me_2SO$, (c) *exo*-$Me_4$,*endo*-$Me_4$-$[(BF_4)_2@Pd_4L_8](BF_4)_6$·$4Me_2SO$, (d) *endo*-$Me_8$-$[(BF_4)_2@Pd_4L_8](BF_4)_8$·$5Me_2SO$, (e) *exo*-$Me_4$,*endo*-$Me_4$-$[(ClO_4)_2@Pd_4L_8]$ $(ClO_4)_6$·$5Me_2SO$, (f) *endo*-Me_8-$[(ClO_4)_2@Pd_4L_8](ClO_4)_6$·$5Me_2SO$, (g) *endo*-$Me_8$-$[(NO_3)_2@$ $Pd_4L_8](PF_6)_6$·$4Me_2SO$, (h) *endo*-Me_8-$[(NO_3)_2@Pd_4L_8](CF_3SO_3)_6$·$2Me_2SO$.

	endo-Me_8-$[(NO_3)_2@Pd_4L_8](NO_3)_6$·5 Me_2SO	*exo*-Me_4-*endo*-Me_4-$[(NO_3)_2@Pd_4L_8](NO_3)_6$·4 Me_2SO	*exo*-Me_4,*endo*-Me_4-$[(BF_4)_2@Pd_4L_8](BF_4)_6$·4M e_2SO	*endo*-Me_8-$[(BF_4)_2@Pd_4L_8](BF_4)_8$·5M e_2SO
Formula	$C_{138}H_{182}N_{24}O_{25}Pd_4SSi_8$	$C_{136}H_{176}N_{24}O_{24}Pd_4Si_8$	$C_{136}H_{176}B_8F_{32}N_{16}Pd_4Si_8$	$C_{146}H_{206}B_8F_{32}N_{16}O_5Pd_4S_5Si_8$
M_w	3259.45	3181.32	3379.72	3770.36
Cryst. sys.	Monoclinic	Orthorhombic	Triclinic	Triclinic
Space group	*C*2/*m*	$P2_12_12$	*P*-1	*P*-1
a/Å	29.5695(7)	33.763(7)	18.542(4)	17.968(4)
b/Å	20.0007(7)	25.417(5)	22.252(4)	18.783(4)
c/Å	16.8654(4)	25.901(5)	27.335(5)	20.866(4)
V/Å^3	9677.3(5)	22227(8)	10288(4)	5919(3)
Z	2	4	2	1
ρ/g cm^{-3}	1.531	0.951	1.091	1.058
μ/mm^{-1}	0.484	0.557	0.523	0.425
R_{int}	0.0550	0.0629	0.0418	0.0506
GoF on F^2	1.076	0.846	1.988	1.075
R_1 [$I>2\sigma(I)$][a]	0.1120	0.0732	0.1402	0.0906
wR_2 (all data)[b]	0.3258	0.2309	0.4087	0.2966

[a]$R1 = \Sigma||F_o| - |F_c||/\Sigma|F_o|$, [b]$wR_2 = (\Sigma[w(F_o^2 - F_c^2)^2]/\Sigma[w(F_o^2)^2])^{1/2}$

	exo-Me_4-*endo*-Me_4-$[(ClO_4)_2@Pd_4L_8](ClO_4)_8$·5 Me_2SO	*endo*-Me_8-$[(ClO_4)_2@Pd_4L_8](ClO_4)_6$· $5Me_2SO$	*endo*-Me_8-$[(NO_3)_2@Pd_4L_8](PF_6)_6$· $4Me_2SO$	*endo*-Me_8-$[(NO_3)_2@Pd_4L_8](CF_3SO_3)_6$ $·2Me_2SO$
Formula	$C_{136}H_{176}Cl_8N_{16}O_{32}Pd_4Si_8$	$C_{140}H_{188}Cl_8N_{16}O_{34}Pd_4S_2$ Si_8	$C_{144}H_{200}F_{36}N_{18}O_{10}P_6Pd_4S_4Si_8$	$C_{142}H_{176}F_{18}N_{18}O_{24}Pd_4S_6Si_8$
M_w	3480.84	3637.09	3991.59	3703.68
Cryst. sys.	Rhombohedral	Triclinic	Monoclinic	Triclinic
Space group	$P2_1/c$	*P*-1	$P2_1/n$	*P*-1
a/Å	33.458(7)	18.335(4)	18.260(4)	18.072(4)
b/Å	17.790(4)	19.458(4)	18.337(4)	18.561(4)
c/Å	35.572(7)	20.980(4)	33.391(7)	18.661(4)
V/Å^3	20930(7)	6257(3)	12866.1(7)	4758(2)
Z	4	1	2	1
ρ/g cm^{-3}	1.105	0.965	1.186	1.293
μ/mm^{-1}	0.738	0.447	0.488	0.439
R_{int}	0.1598	0.0372	0.1347	0.0371
GoF on F^2	1.159	1.395	0.934	1.140
R_1 [$I>2\sigma(I)$][a]	0.0988	0.1030	0.0767	0.0674
wR_2 (all data)[b]	0.2898	0.3446	0.2355	0.1998

[a]$R1 = \Sigma||F_o| - |F_c||/\Sigma|F_o|$, [b]$wR_2 = (\Sigma[w(F_o^2 - F_c^2)^2]/\Sigma[w(F_o^2)^2])^{1/2}$

Table S3. Crystal Data and Refinement Parameters for (a) *endo*-Me_8-$[(NO_3)_2@Pd_4L_8](NO_3)_6 \cdot 5Me_2SO$, (b) *exo*-$Me_4$-*endo*-$Me_4$-$[(NO_3)_2@Pd_4L_8](NO_3)_6 \cdot 4Me_2SO$, (c) *exo*-$Me_4$,*endo*-$Me_4$-$[(BF_4)_2@Pd_4L_8](BF_4)_6 \cdot 4Me_2SO$, (d) *endo*-$Me_8$-$[(BF_4)_2@Pd_4L_8](BF_4)_8 \cdot 5Me_2SO$, (e) *exo*-$Me_4$,*endo*-$Me_4$-$[(ClO_4)_2@Pd_4L_8]$ $(ClO_4)_6 \cdot 5Me_2SO$, (f) *endo*-Me_8-$[(ClO_4)_2@Pd_4L_8](ClO_4)_6 \cdot 5Me_2SO$, (g) *endo*-$Me_8$-$[(NO_3)_2@$ $Pd_4L_8](PF_6)_6 \cdot 4Me_2SO$, (h) *endo*-$Me_8$-$[(NO_3)_2@Pd_4L_8](CF_3SO_3)_6 \cdot 2Me_2SO$.

endo-Me_8-$[(NO_3)_2@Pd_4L_8](NO_3)_6{\cdot}5Me_2SO$		*exo*-Me_4-*endo*-Me_4-$[(NO_3)_2@Pd_4L_8](NO_3)_6{\cdot}4Me_2SO$		*exo*-Me_4,*endo*-Me_4-$[(BF_4)_2@Pd_4L_8](BF_4)_6{\cdot}4Me_2SO$		*endo*-Me_8-$[(BF_4)_2@Pd_4L_8](BF_4)_8{\cdot}5Me_2SO$	
Pd(1)-N(8A)$^{\#1}$	2.005(4)	Pd(1)-N(2C)	2.001(13)	Pd(1)-N(1A)	2.013(4)	Pd(1)-N(1C)	2.018(4)
Pd(1)-N(1A)	2.005(4)	Pd(1)-N(2A)	2.030(11)	Pd(1)-N(1C)	2.016(4)	Pd(1)-N(1A)	2.026(4)
Pd(1)-N(41A)	2.008(7)	Pd(1)-N(2B)	2.034(12)	Pd(1)-N(1B)	2.018(5)	Pd(1)-N(1B)	2.032(4)
Pd(1)-N(21A)	2.014(4)	Pd(1)-N(9C)$^{\#1}$	2.037(12)	Pd(1)-N(1D)	2.031(5)	Pd(1)-N(1D)	2.049(4)
		Pd(2)-N(9D)$^{\#1}$	1.994(11)	Pd(2)-N(1H)	2.019(5)	Pd(2)-N(8D)	2.027(4)
N(8A)$^{\#1}$-Pd(1)-N(1A)	91.6(3)	Pd(2)-N(9A)	2.013(11)	Pd(2)-N(1G)	2.020(5)	Pd(2)-N(8C)	2.027(4)
N(8A)$^{\#1}$-Pd(1)-N(41A)	89.9(3)	Pd(2)-N(9B)	2.042(10)	Pd(2)-N(8A)	2.028(5)	Pd(2)-N(8B)$^{\#1}$	2.033(4)
N(1A)-Pd(1)-N(41A)	177.3(2)	Pd(2)-N(2D)	2.067(10)	Pd(2)-N(8B)	2.071(5)	Pd(2)-N(8A)$^{\#1}$	2.037(4)
N(8A)$^{\#1}$-Pd(1)-N(21A)	177.1(2)	Pd(3)-N(2E)	2.012(12)	Pd(3)-N(8D)	1.971(6)		
N(1A)-Pd(1)-N(21A)	89.3(3)	Pd(3)-N(9G)$^{\#2}$	2.013(12)	Pd(3)-N(8C)	1.965(6)	N(1C)-Pd(1)-N(1A)	90.38(17)
N(41A)-Pd(1)-N(21A)	89.1(3)	Pd(3)-N(2G)	2.038(12)	Pd(3)-N(1F)	1.993(6)	N(1C)-Pd(1)-N(1B)	178.25(16)
		Pd(3)-N(2F)	2.043(12)	Pd(3)-N(1E)	2.072(7)	N(1A)-Pd(1)-N(1B)	90.81(19)
				Pd(4)-N(8E)	1.973(6)	N(1C)-Pd(1)-N(1D)	91.01(16)
		Pd(1)-N(2C)	2.001(13)	Pd(4)-N(8F)	2.016(6)	N(1A)-Pd(1)-N(1D)	178.58(16)
		Pd(1)-N(2A)	2.030(11)	Pd(4)-N(8G)	2.018(6)	N(1B)-Pd(1)-N(1D)	87.80(18)
		Pd(1)-N(2B)	2.034(12)	Pd(4)-N(8H)	2.019(6)	N(8D)-Pd(2)-N(8C)	89.42(18)
		Pd(1)-N(9C)$^{\#1}$	2.037(12)			N(8D)-Pd(2)-N(8B)$^{\#1}$	178.38(16)
		Pd(2)-N(9D)$^{\#1}$	1.994(11)	Pd(1)-N(1A)	2.013(4)	N(8C)-Pd(2)-N(8B)$^{\#1}$	89.52(17)
		Pd(2)-N(9A)	2.013(11)	Pd(1)-N(1C)	2.016(4)	N(8D)-Pd(2)-N(8A)$^{\#1}$	89.13(18)
		Pd(2)-N(9B)	2.042(10)	Pd(1)-N(1B)	2.018(5)	N(8C)-Pd(2)-N(8A)$^{\#1}$	178.27(18)
		Pd(2)-N(2D)	2.067(10)	Pd(1)-N(1D)	2.031(5)	N(8B)$^{\#1}$-Pd(2)-N(8A)$^{\#1}$	91.95(17)
		Pd(3)-N(2E)	2.012(12)	Pd(2)-N(1H)	2.019(5)		
		Pd(3)-N(9G)$^{\#2}$	2.013(12)	Pd(2)-N(1G)	2.020(5)		
		Pd(3)-N(2G)	2.038(12)	Pd(2)-N(8A)	2.028(5)		
		Pd(3)-N(2F)	2.043(12)	Pd(2)-N(8B)	2.071(5)		
		Pd(1)-N(2C)	2.001(13)	Pd(3)-N(8D)	1.971(6)		
		Pd(1)-N(2A)	2.030(11)	Pd(3)-N(8C)	1.965(6)		
		Pd(1)-N(2B)	2.034(12)	Pd(3)-N(1F)	1.993(6)		
		Pd(1)-N(9C)$^{\#1}$	2.037(12)	Pd(3)-N(1E)	2.072(7)		
		Pd(2)-N(9D)$^{\#1}$	1.994(11)	Pd(4)-N(8E)	1.973(6)		
		Pd(2)-N(9A)	2.013(11)	Pd(4)-N(8F)	2.016(6)		
				Pd(4)-N(8G)	2.018(6)		
				Pd(4)-N(8H)	2.019(6)		
				Pd(1)-N(1A)	2.013(4)		
				Pd(1)-N(1C)	2.016(4)		
				Pd(1)-N(1B)	2.018(5)		
				Pd(1)-N(1D)	2.031(5)		
				Pd(2)-N(1H)	2.019(5)		
				Pd(2)-N(1G)	2.020(5)		
				Pd(2)-N(8A)	2.028(5)		
				Pd(2)-N(8B)	2.071(5)		

$^{\#1}$ $-x+1,y,-z$

$^{\#1}$ $-x+1,-y+1,z$
$^{\#2}$ $-x+1,-y,z$

$^{\#1}$ $-x+1,-y+2,-z+1$

exo-Me_4-*endo*-Me_4-$[(ClO_4)_2@Pd_4L_8](ClO_4)_8{\cdot}5Me_2SO$		*endo*-Me_8-$[(ClO_4)_2@Pd_4L_8](ClO_4)_6{\cdot}5Me_2SO$		*exo*-Me_4,*endo*-Me_4-$[(BF_4)_2@Pd_4L_8](BF_4)_6{\cdot}4Me_2SO$		*endo*-Me_8-$[(NO_3)_2@Pd_4L_8](CF_3SO_3)_6{\cdot}2Me_2SO$	
Pd(1)-N(1A)	2.009(9)	Pd(1)-N(3)	2.021(5)	N(4)-Pd(1)$^{\#1}$	2.018(4)	Pd(1)-N(6)#1	2.017(3)
Pd(1)-N(1D)	2.035(9)	Pd(1)-N(5)	2.027(5)	N(8)-Pd(1)	2.029(3)	Pd(1)-N(7)	2.019(3)
Pd(1)-N(1B)	2.040(10)	Pd(1)-N(1)	2.028(5)	N(7)-Pd(2)	2.036(3)	Pd(1)-N(3)	2.027(3)
Pd(1)-N(1C)	2.048(10)	Pd(1)-N(8)$^{\#1}$	2.041(5)	N(6)-Pd(1)$^{\#1}$	2.030(3)	Pd(1)-N(1)	2.030(3)
Pd(2)-N(8A)	1.972(10)	Pd(3)-N(6)	2.019(4)	N(5)-Pd(2)	2.024(4)	N(5)-Pd(2)	2.021(3)
Pd(2)-N(1E)	2.015(10)	Pd(3)-N(2)$^{\#1}$	2.029(4)	Pd(1)-N(1)	2.022(4)		
Pd(2)-N(1F)	2.022(9)	Pd(3)-N(7)	2.047(5)	Pd(2)-Br(3)	2.421(2)	N(6)$^{\#1}$-Pd(1)-N(7)	88.31(14)
Pd(2)-N(8B)	2.046(9)	Pd(3)-N(4)	2.050(4)	Pd(2)-Br(4)	2.437(2)	N(6)$^{\#1}$-Pd(1)-N(3)	177.43(12)
Pd(3)-N(1H)	2.022(11)					N(7)-Pd(1)-N(3)	90.75(13)
Pd(3)-N(1G)	2.025(10)	N(3)-Pd(1)-N(5)	89.35(19)	N(4)$^{\#1}$-Pd(1)-N(1)	177.57(14)	N(6)$^{\#1}$-Pd(1)-N(1)	93.17(14)
Pd(3)-N(8F)	2.026(10)	N(3)-Pd(1)-N(1)	178.64(16)	N(4)$^{\#1}$-Pd(1)-N(8)	86.28(15)	N(7)-Pd(1)-N(1)	177.28(12)
Pd(3)-N(8E)	2.027(9)	N(5)-Pd(1)-N(1)	89.53(18)	N(1)-Pd(1)-N(8)	94.88(15)	N(3)-Pd(1)-N(1)	87.68(13)
Pd(4)-N(8D)	2.013(11)	N(3)-Pd(1)-N(8)$^{\#1}$	89.6(2)	N(4)$^{\#1}$-Pd(1)-N(6)$^{\#1}$	90.25(15)	N(4)-Pd(2)-N(5)	89.55(12)
Pd(4)-N(8H)	2.030(10)	N(5)-Pd(1)-N(8)$^{\#1}$	178.68(18)	N(1)-Pd(1)-N(6)$^{\#1}$	88.58(15)	N(4)-Pd(2)-N(8)	87.26(11)
Pd(4)-N(8C)	2.029(9)	N(1)-Pd(1)-N(8)$^{\#1}$	91.57(19)	N(8)-Pd(1)-N(6)$^{\#1}$	176.51(16)	N(5)-Pd(2)-N(8)	175.92(12)
Pd(4)-N(8G)	2.040(11)	N(6)-Pd(3)-N(2)$^{\#1}$	178.57(16)	N(2)-Pd(2)-N(5)	177.59(14)	N(4)-Pd(2)-N(2)$^{\#1}$	177.69(11)
		N(6)-Pd(3)-N(7)	90.43(18)	N(2)-Pd(2)-N(3)	90.27(15)	N(5)-Pd(2)-N(2)$^{\#1}$	90.90(12)
N(1A)-Pd(1)-N(1D)	175.9(4)	N(2)$^{\#1}$-Pd(3)-N(7)	90.43(19)	N(5)-Pd(2)-N(3)	87.67(15)	N(8)-Pd(2)-N(2)$^{\#1}$	92.19(12)
N(1A)-Pd(1)-N(1B)	92.4(4)	N(6)-Pd(3)-N(4)	90.14(18)	N(2)-Pd(2)-N(7)	91.10(15)	N(7)-Pd(2)-Br(3)	90(4)
N(1D)-Pd(1)-N(1B)	91.6(4)	N(2)$^{\#1}$-Pd(3)-N(4)	89.01(19)	N(5)-Pd(2)-N(7)	90.91(15)	N(7)-Pd(2)-Br(4)	90(4)
N(1A)-Pd(1)-N(1C)	87.3(4)	N(7)-Pd(3)-N(4)	179.36(17)	N(3)-Pd(2)-N(7)	177.58(15)	Br(3)-Pd(2)-Br(4)	175.6(9)
N(1D)-Pd(1)-N(1C)	88.8(4)						
N(1B)-Pd(1)-N(1C)	179.1(4)						
N(8A)-Pd(2)-N(1E)	177.8(4)						
N(8A)-Pd(2)-N(1F)	91.1(4)						
N(1E)-Pd(2)-N(1F)	88.9(4)						
N(8A)-Pd(2)-N(8B)	91.5(4)						
N(1E)-Pd(2)-N(8B)	88.7(4)						
N(1F)-Pd(2)-N(8B)	175.1(4)						
N(1H)-Pd(3)-N(1G)	92.1(4)						
N(1H)-Pd(3)-N(8F)	178.0(4)						
N(1G)-Pd(3)-N(8F)	87.8(4)						
N(1H)-Pd(3)-N(8E)	91.8(4)						
N(1G)-Pd(3)-N(8E)	175.3(4)						
N(8F)-Pd(3)-N(8E)	88.4(4)						
N(8D)-Pd(4)-N(8H)	89.2(4)						
N(8D)-Pd(4)-N(8C)	87.1(4)						
N(8H)-Pd(4)-N(8C)	175.9(4)						
N(8D)-Pd(4)-N(8G)	177.1(5)						
N(8H)-Pd(4)-N(8G)	91.0(4)						
N(8C)-Pd(4)-N(8G)	92.8(4)						

$^{\#1}$ $-x+1,-y+1,-z+1$ $^{\#1}$ $-x+1,-y+1,-z+1$ $^{\#1}$ $-x+1,-y,-z+1$

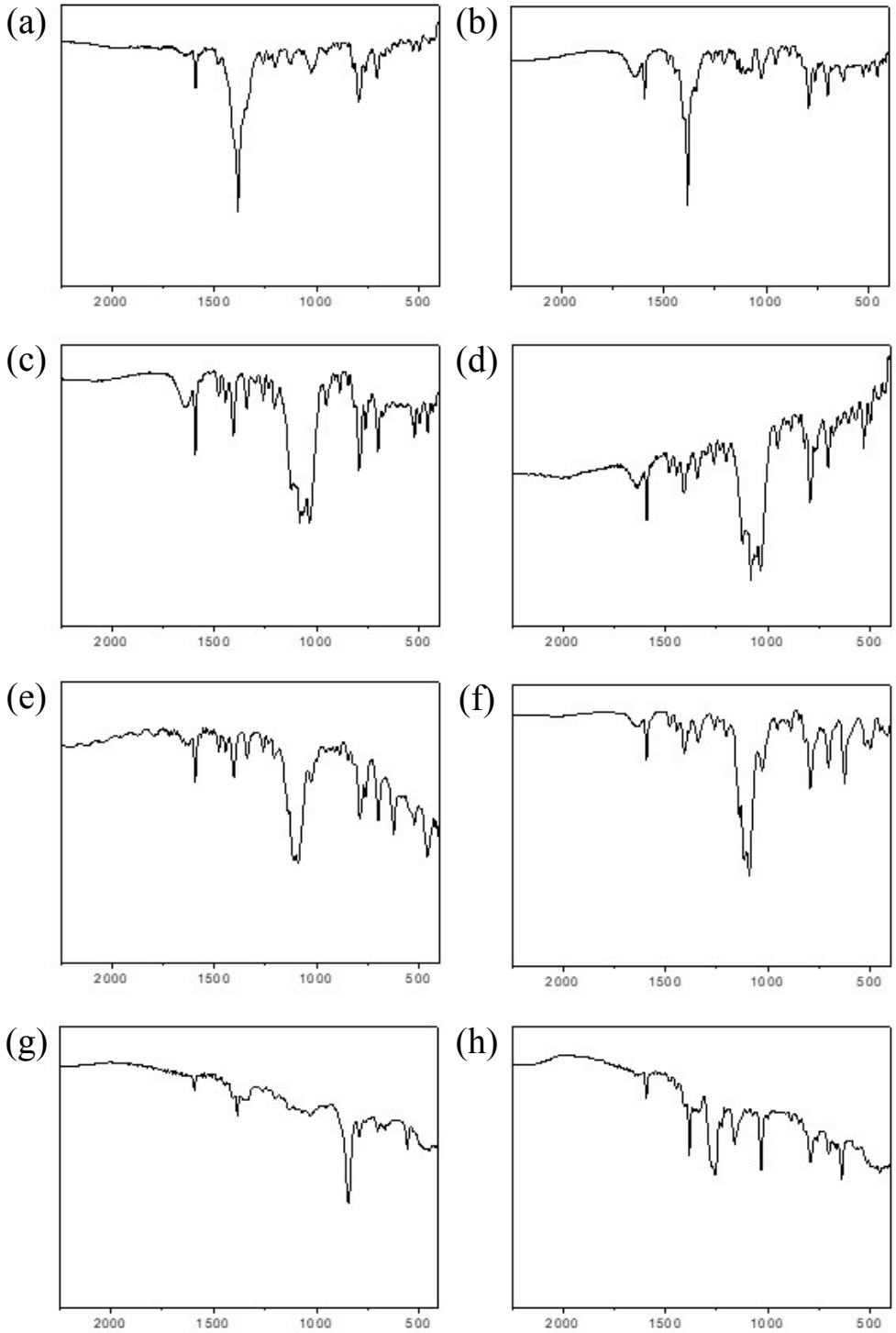

Fig. S1 FT-IR Spectra of (a) *endo*-Me_8-[$(NO_3)_2$@Pd_4L_8]$(NO_3)_6$·$5Me_2SO$, (b) *exo*-Me_4-*endo*-Me_4-[$(NO_3)_2$@Pd_4L_8]$(NO_3)_6$·$4Me_2SO$, (c) *exo*-Me_4,*endo*-Me_4-[$(BF_4)_2$@Pd_4L_8]$(BF_4)_6$·$4Me_2SO$, (d) *endo*-Me_8-[$(BF_4)_2$@Pd_4L_8]$(BF_4)_8$·$5Me_2SO$, (e) *exo*-Me_4,*endo*-Me_4-[$(ClO_4)_2$@Pd_4L_8] $(ClO_4)_6$·$5Me_2SO$, (f) *endo*-Me_8-[$(ClO_4)_2$@Pd_4L_8]$(ClO_4)_6$·$5Me_2SO$, (g) *endo*-Me_8-[$(NO_3)_2$@ Pd_4L_8]$(PF_6)_6$·$4Me_2SO$, (h) *endo*-Me_8-[$(NO_3)_2$@Pd_4L_8]$(CF_3SO_3)_6$·$2Me_2SO$.

(a)

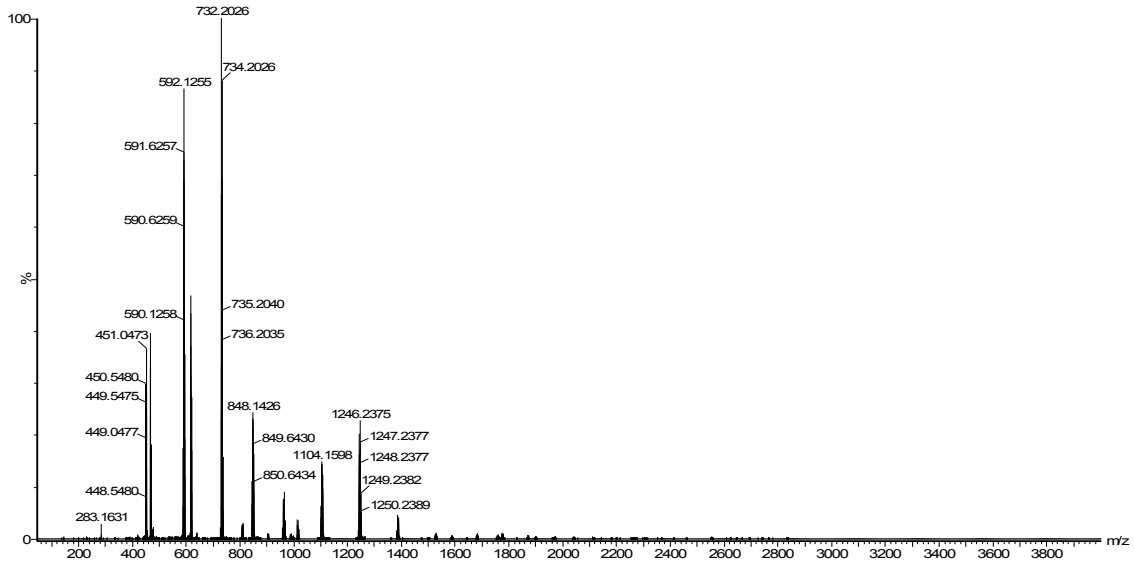
100
%
0
732.2026
734.2026
592.1255
591.6257
590.6259
735.2040
590.1258
736.2035
451.0473
450.5480
449.5475
848.1426
1246.2375
449.0477
849.6430
1247.2377
1104.1598
1248.2377
850.6434
1249.2382
448.5480
1250.2389
283.1631
200 400 600 800 1000 1200 1400 1600 1800 2000 2200 2400 2600 2800 3000 3200 3400 3600 3800
m/z

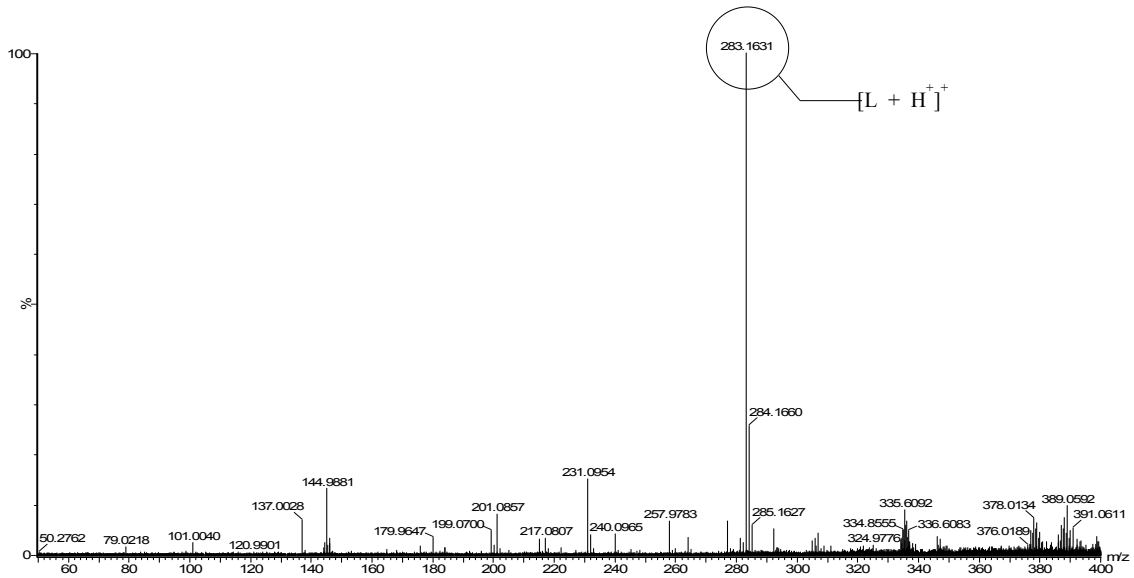
100
%
0
283.1631
[L + H+]+
284.1660
231.0954
144.9881
137.0028
201.0857
335.6092
378.0134
389.0592
391.0611
257.9783
285.1627
199.0700
179.9647
217.0807
240.0965
334.8555
336.6083
376.0189
324.9776
50.2762
79.0218
101.0040
120.9901
60 80 100 120 140 160 180 200 220 240 260 280 300 320 340 360 380 400
m/z

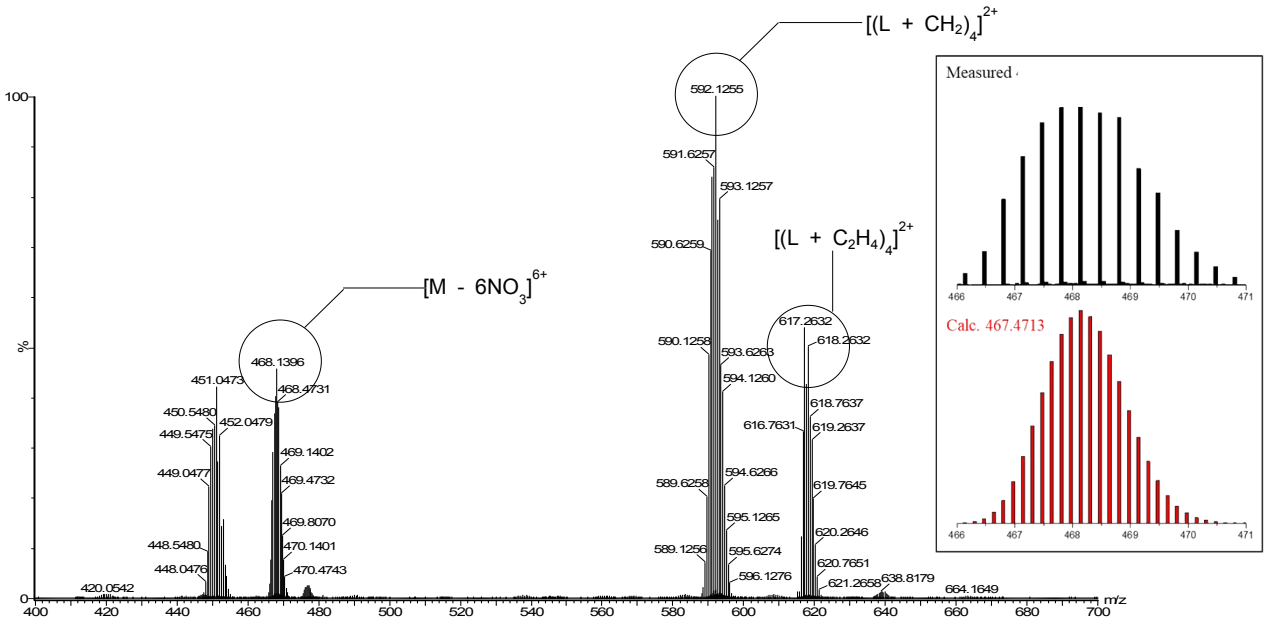
[(L + CH2)4]2+
[(L + C2H4)4]2+
[M - 6NO3]6+
592.1255
591.6257
593.1257
590.6259
590.1258
593.6263
594.1260
589.6258
594.6266
589.1256
595.1265
595.6274
596.1276
617.2632
618.2632
618.7637
616.7631
619.2637
619.7645
620.2646
620.7651
621.2658
638.8179
664.1649
468.1396
468.4731
451.0473
450.5480
452.0479
449.5475
469.1402
449.0477
469.4732
469.8070
448.5480
470.1401
448.0476
470.4743
420.0542
Measured
Calc. 467.4713
100
%
0
m/z

(b)

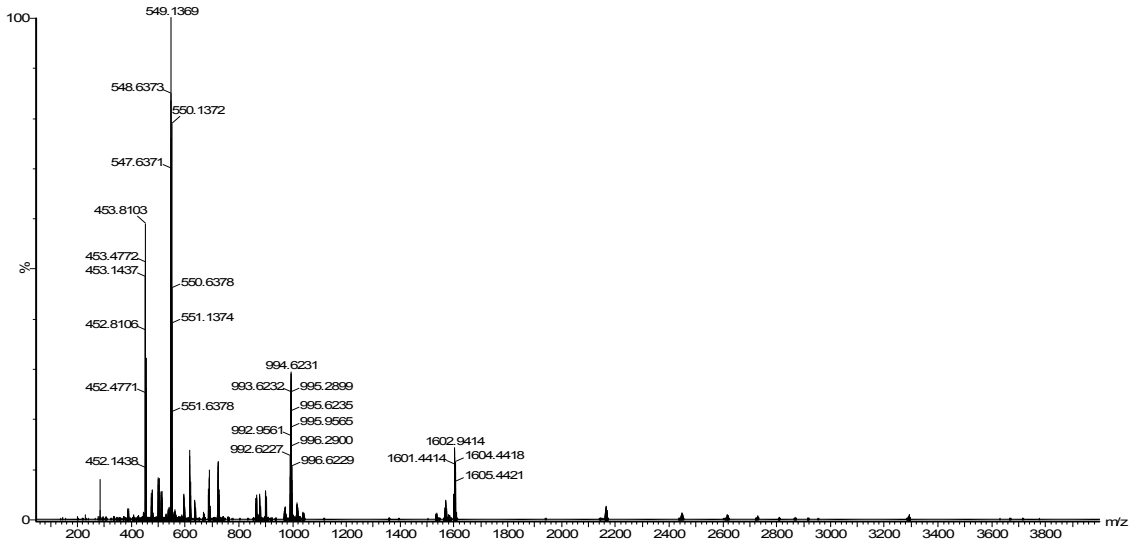
549.1369
548.6373
550.1372
547.6371
453.8103
453.4772
453.1437
550.6378
551.1374
452.8106
994.6231
452.4771
993.6232
995.2899
995.6235
551.6378
995.9565
992.9561
996.2900
992.6227
996.6229
452.1438
1602.9414
1601.4414
1604.4418
1605.4421
100
%
0
m/z

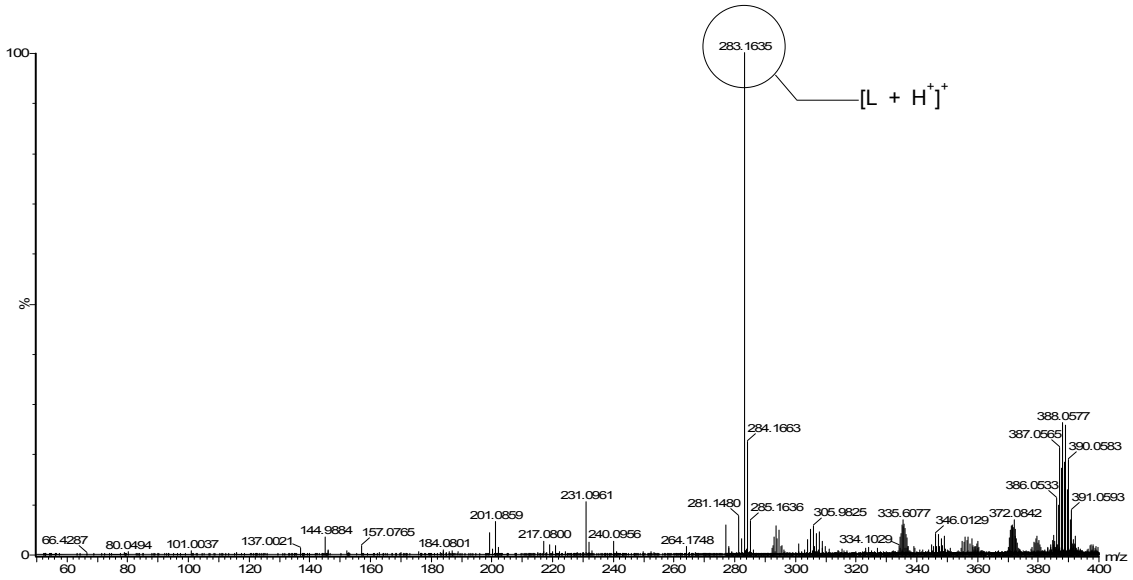
283.1635
[L + H+]+
284.1663
388.0577
387.0565
390.0583
386.0533
391.0593
231.0961
281.1480
285.1636
305.9825
335.6077
346.0129
372.0842
201.0859
217.0800
240.0956
264.1748
334.1029
144.9884
157.0765
66.4287
80.0494
101.0037
137.0021
184.0801
%
m/z

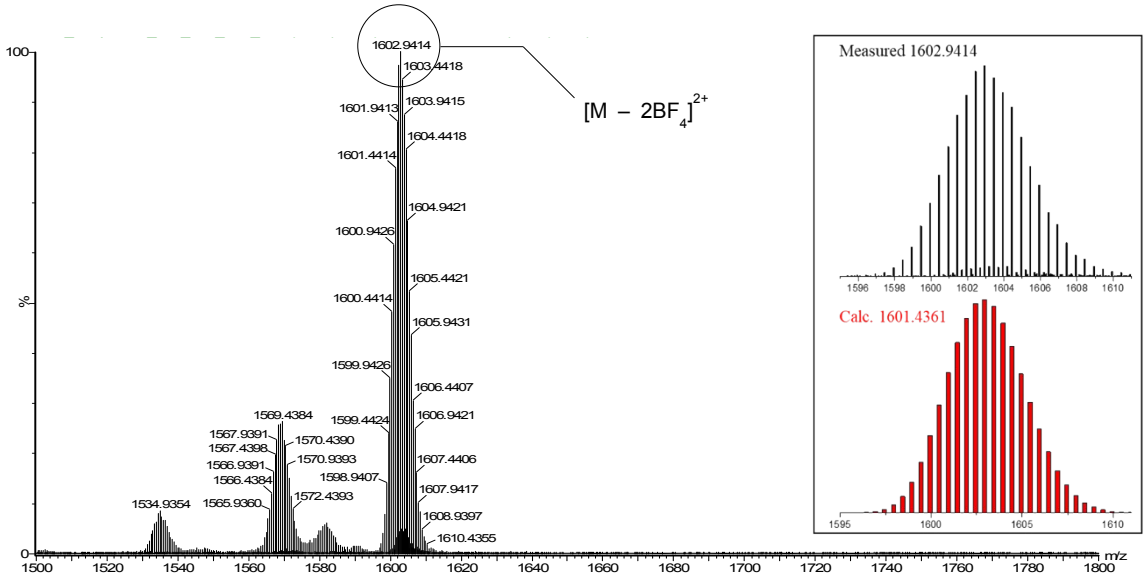
1602.9414
[M – 2BF4]2+
1603.4418
1601.9413
1603.9415
1604.4418
1601.4414
1604.9421
1600.9426
1605.4421
1600.4414
1605.9431
1599.9426
1606.4407
1569.4384
1599.4424
1606.9421
1567.9391
1567.4398
1570.4390
1570.9393
1607.4406
1566.9391
1598.9407
1566.4384
1607.9417
1534.9354
1565.9360
1572.4393
1608.9397
1610.4355
%
m/z
Measured 1602.9414
Calc. 1601.4361

(c)

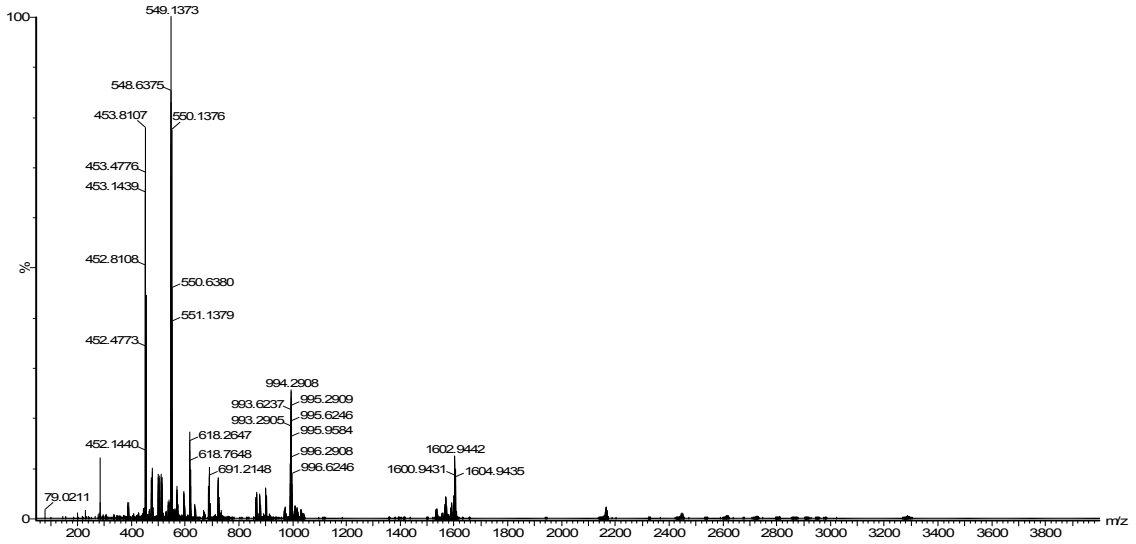
549.1373
548.6375
453.8107
550.1376
453.4776
453.1439
452.8108
550.6380
551.1379
452.4773
994.2908
993.6237
995.2909
993.2905
995.6246
995.9584
618.2647
452.1440
618.7648
996.2908
691.2148
996.6246
1602.9442
1600.9431
1604.9435
79.0211
%
m/z

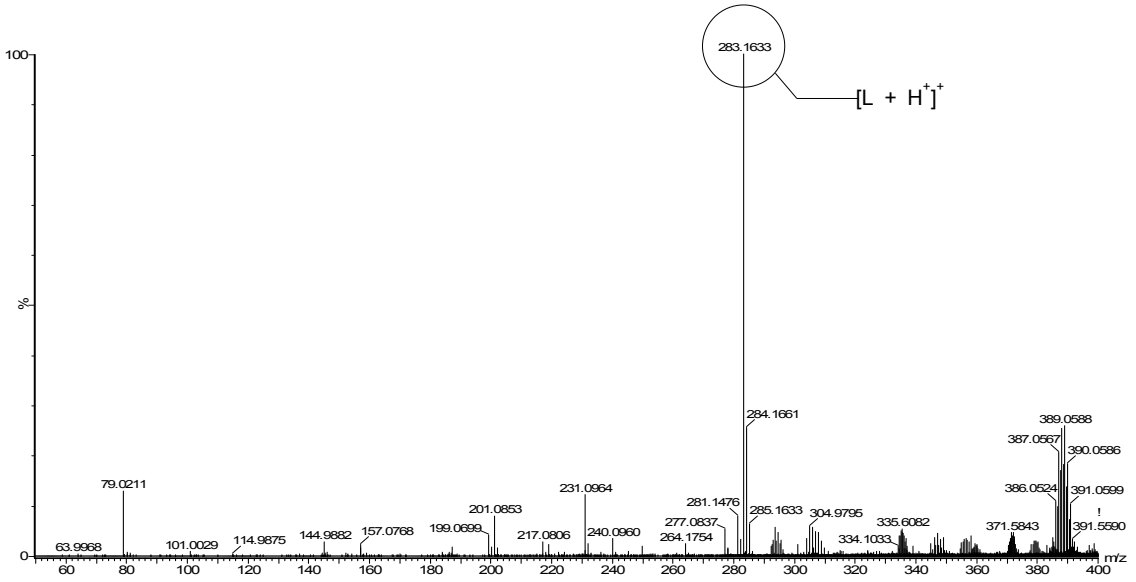
283.1633
[L + H+]+
284.1661
389.0588
387.0567
390.0586
79.0211
231.0964
386.0524
391.0599
281.1476
201.0853
285.1633
304.9795
277.0837
335.6082
371.5843
391.5590
199.0699
240.0960
264.1754
334.1033
63.9968
101.0029
114.9875
144.9882
157.0768
217.0806
%
m/z

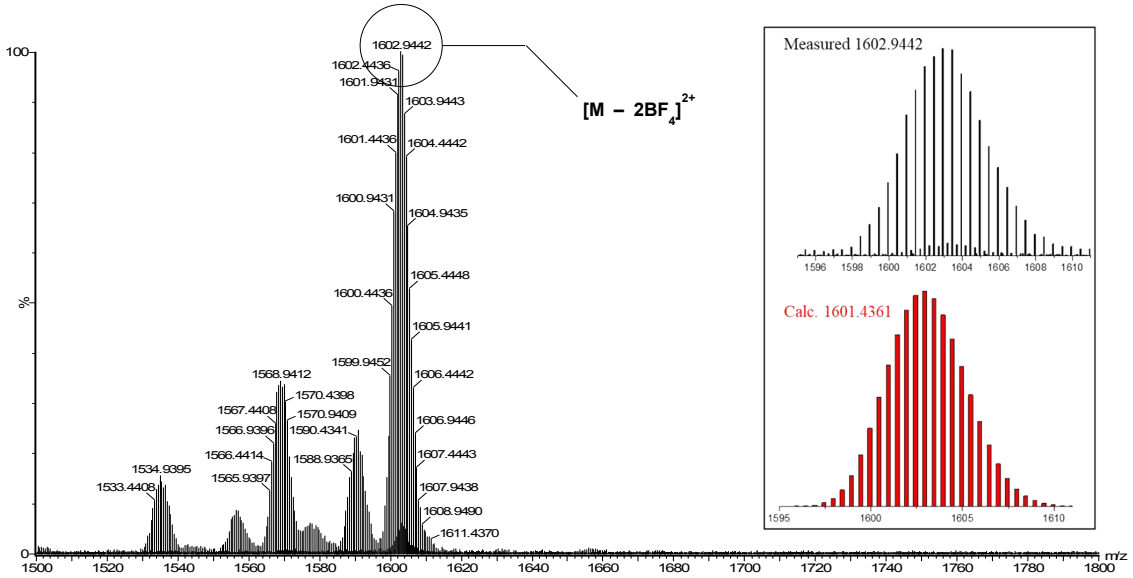

Fig. S2 ESI-Mass data of (a) *endo*-Me_8-[$(NO_3)_2$@Pd_4L_8]$(NO_3)_6$·5Me_2SO, (b) *exo*-Me_4,*endo*-Me_4-[$(BF_4)_2$@Pd_4L_8]$(BF_4)_6$·4Me_2SO, (c) *endo*-Me_8-[$(BF_4)_2$@Pd_4L_8] $(BF_4)_8$·5Me_2SO.

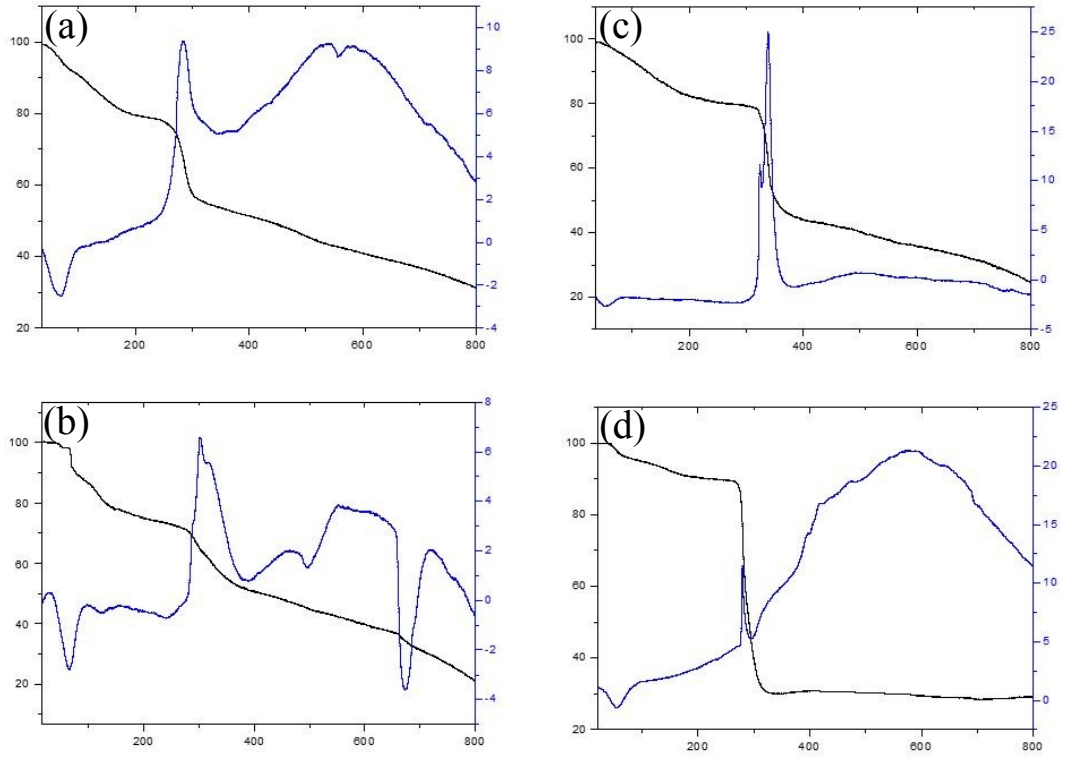

Fig. S3 TGA curves for (a) *endo*-Me_8-[$(NO_3)_2$@Pd_4L_8]$(NO_3)_6$·5Me_2SO, (b) *exo*-Me_4-*endo*-Me_4-[$(NO_3)_2$@Pd_4L_8]$(NO_3)_6$·4Me_2SO, (c) *exo*-Me_4,*endo*-Me_4-[$(BF_4)_2$@Pd_4L_8]$(BF_4)_6$ ·4Me_2SO, (d) *endo*-Me_8-[$(BF_4)_2$@Pd_4L_8]$(BF_4)_8$·5Me_2SO.

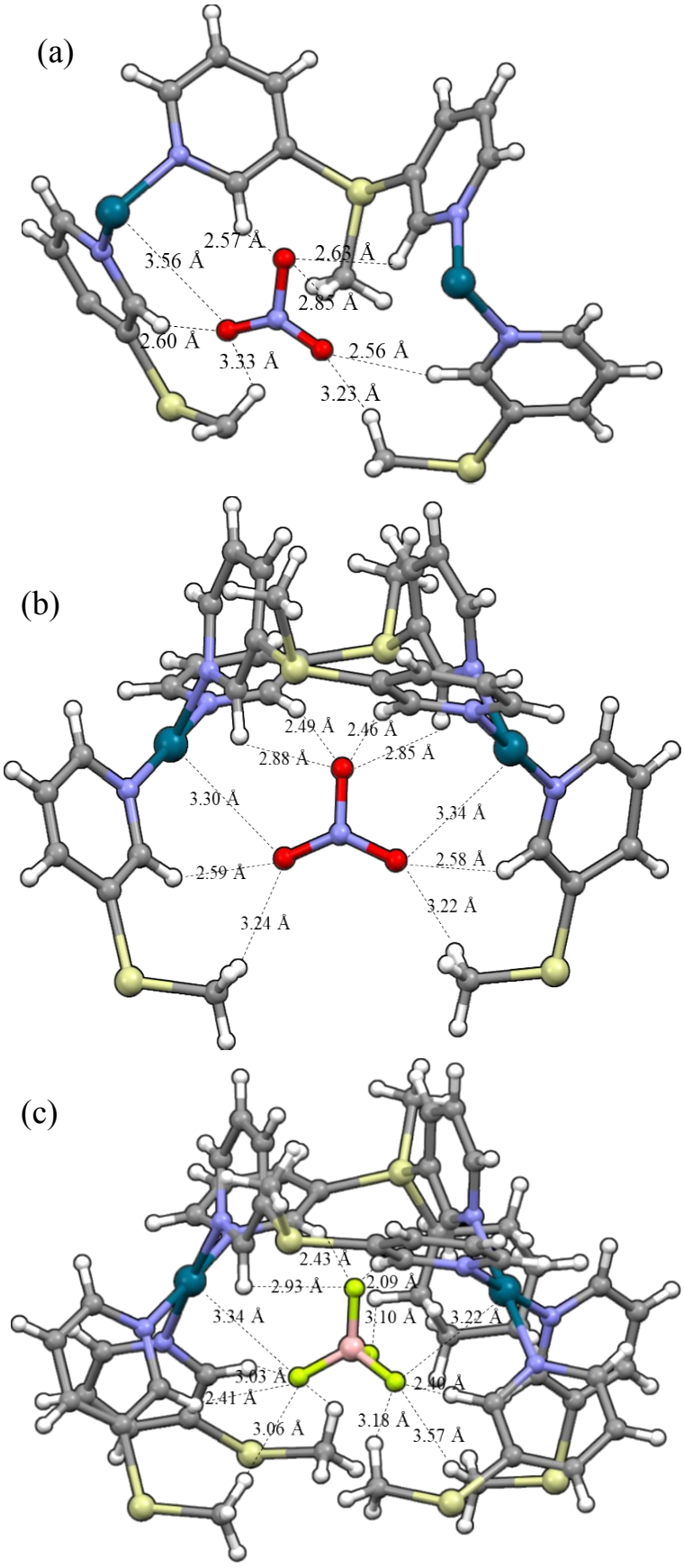
(a)
2.57 Å
2.68 Å
3.56 Å
2.85 Å
2.60 Å
3.33 Å
2.56 Å
3.23 Å
(b)
2.49 Å
2.46 Å
2.88 Å
2.85 Å
3.30 Å
3.34 Å
2.59 Å
2.58 Å
3.22 Å
3.24 Å
(c)
2.43 Å
2.93 Å
2.09 Å
3.34 Å
3.10 Å
3.22 Å
3.03 Å
2.40 Å
2.41 Å
3.06 Å
3.18 Å
3.57 Å

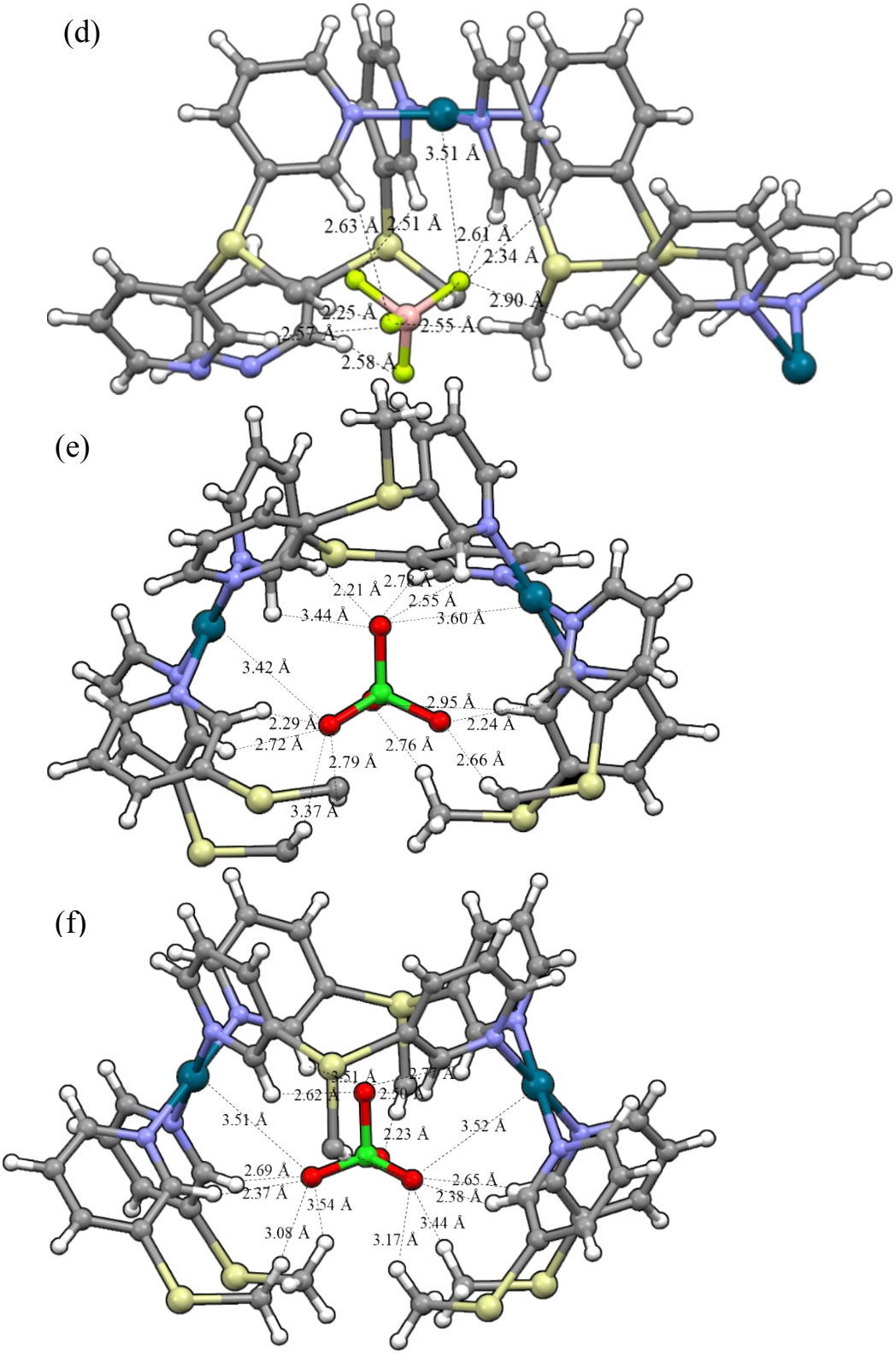

Fig. S4 Interaction distances between inner anion and cage of (a) *endo*-Me_8-$[(NO_3)_2@Pd_4L_8](NO_3)_6{\cdot}5Me_2SO$, (b) *exo*-$Me_4$-*endo*-$Me_4$-$[(NO_3)_2@Pd_4L_8](NO_3)_6{\cdot}4Me_2SO$, (c) *exo*-$Me_4$,*endo*-$Me_4$-$[(BF_4)_2@Pd_4L_8]$ $(BF_4)_6{\cdot}4Me_2SO$, (d) *endo*-Me_8-$[(BF_4)_2@Pd_4L_8](BF_4)_8{\cdot}5Me_2SO$, (e) *exo*-$Me_4$,endo-$Me_4$-$[(ClO_4)_2@Pd_4L_8](ClO_4)_6{\cdot}5Me_2SO$, (f) *endo*-$Me_8$-$[(ClO_4)_2$ $@Pd_4L_8](ClO_4)_6$ $\cdot 5Me_2SO$.

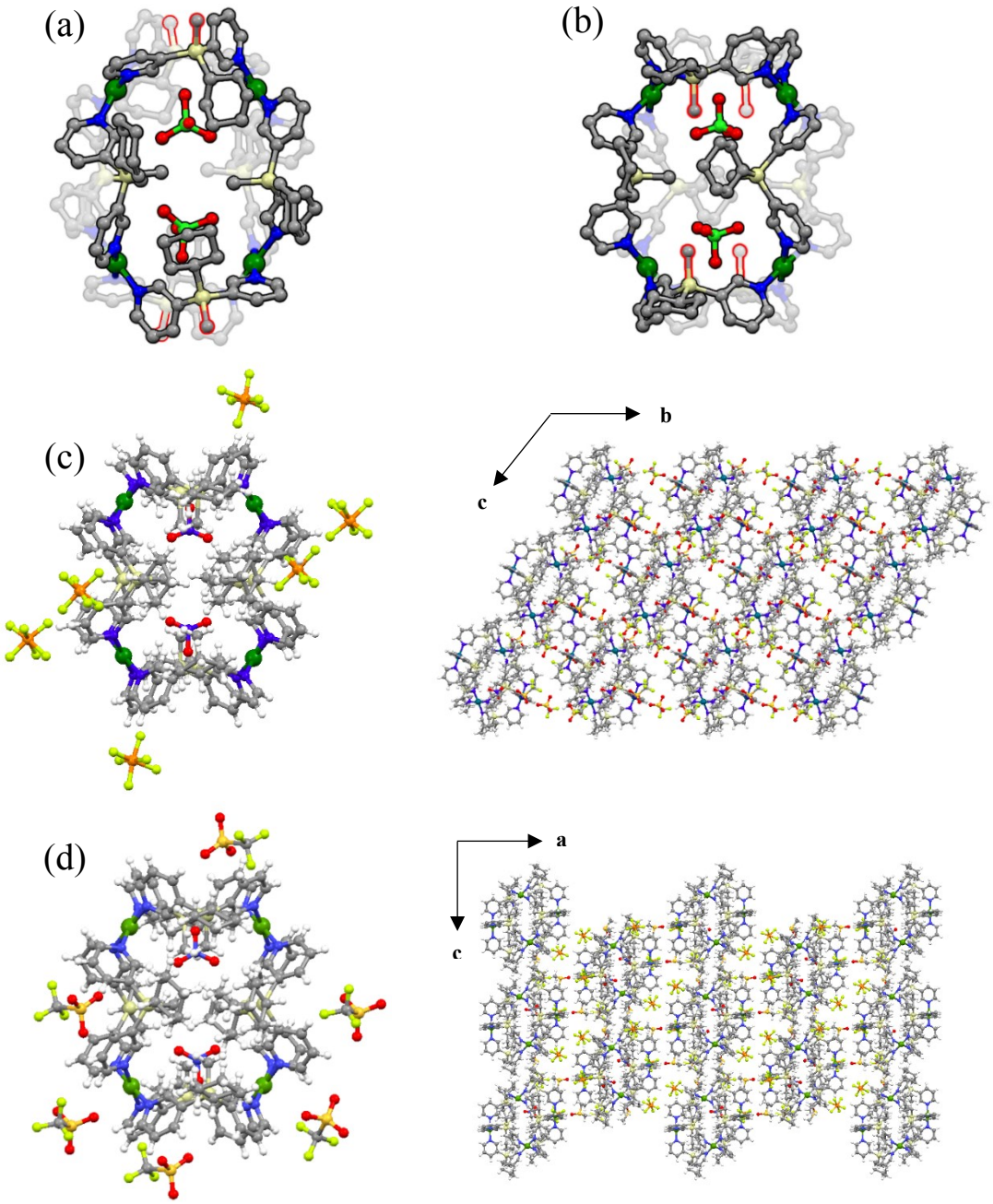

Fig. S5 Crystal structures of (a) *exo*-Me_4,*endo*-Me_4-[$(ClO_4)_2$@Pd_4L_8]$(ClO_4)_6$·5Me_2SO, (b) *endo*-Me_8-[$(ClO_4)_2$@Pd_4L_8]$(ClO_4)_6$·5Me_2SO, (c, left) *endo*-Me_8-[$(NO_3)_2$@Pd_4L_8] $(PF_6)_6$·4Me_2SO, and (c, right) its packing, (d, left) *endo*-Me_8-[$(NO_3)_2$@Pd_4L_8]$(CF_3SO_3)_6$ ·2Me_2SO, (d, right).

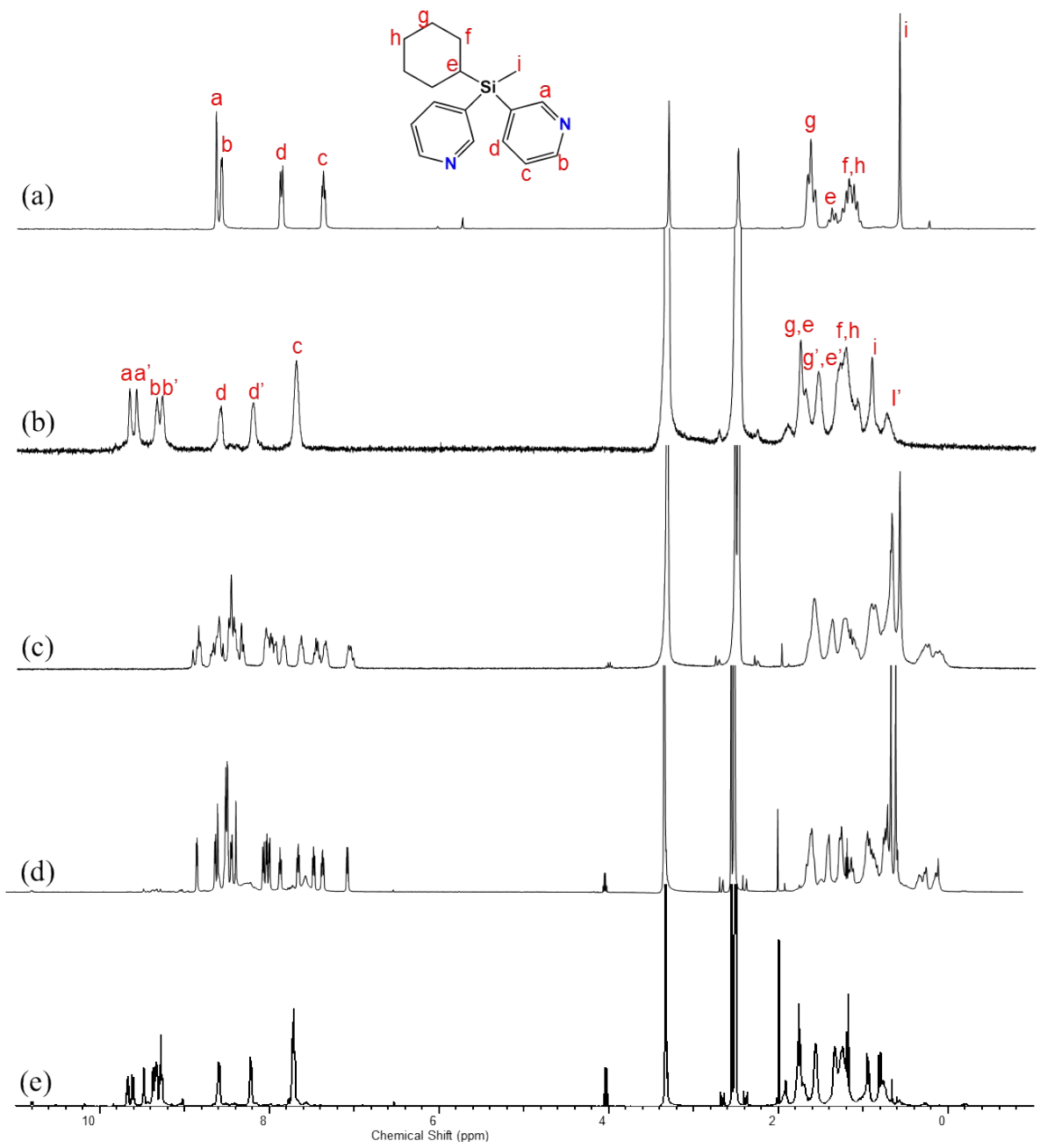
(a)
(b)
(c)
(d)
(e)
a
b
d
c
g
f,h
e
i
aa'
bb'
d'
g,e
g',e'
l'
10
8
6
4
2
0
Chemical Shift (ppm)
Si
N

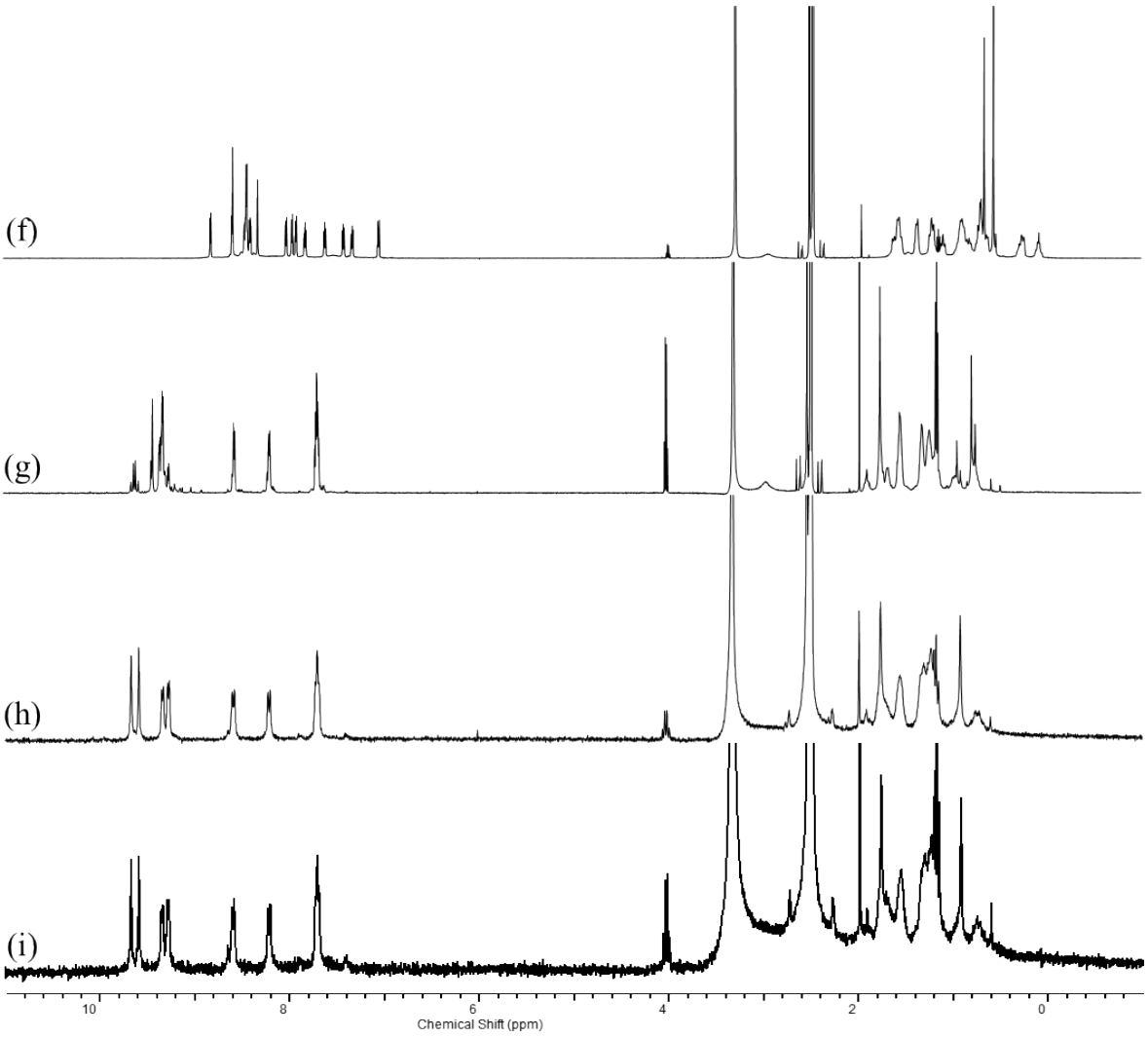

Fig. S6 ^{1}H NMR spectra of (a) L, (b) *endo*-Me_8-[$(NO_3)_2$@Pd_4L_8]$(NO_3)_6$·5Me_2SO, (c) *exo*-Me_4-*endo*-Me_4-[$(NO_3)_2$@Pd_4L_8]$(NO_3)_6$·4Me_2SO, (d) *exo*-Me_4,*endo*-Me_4-[$(BF_4)_2$@Pd_4L_8] $(BF_4)_6$·4Me_2SO, (e) *endo*-Me_8-[$(BF_4)_2$@Pd_4L_8]$(BF_4)_8$·5Me_2SO, (f) *exo*-Me_4,endo-Me_4-[$(ClO_4)_2$@Pd_4L_8]$(ClO_4)_6$·5Me_2SO, (g) *endo*-Me_8-[$(ClO_4)_2$ @Pd_4L_8]$(ClO_4)_6$ ·5Me_2SO, (h) *endo*-Me_8-[$(NO_3)_2$@Pd_4L_8]$(PF_6)_6$·4Me_2SO, (i) *endo*-Me_8-[$(NO_3)_2$@Pd_4L_8] $(CF_3SO_3)_6$ ·2Me_2SO.

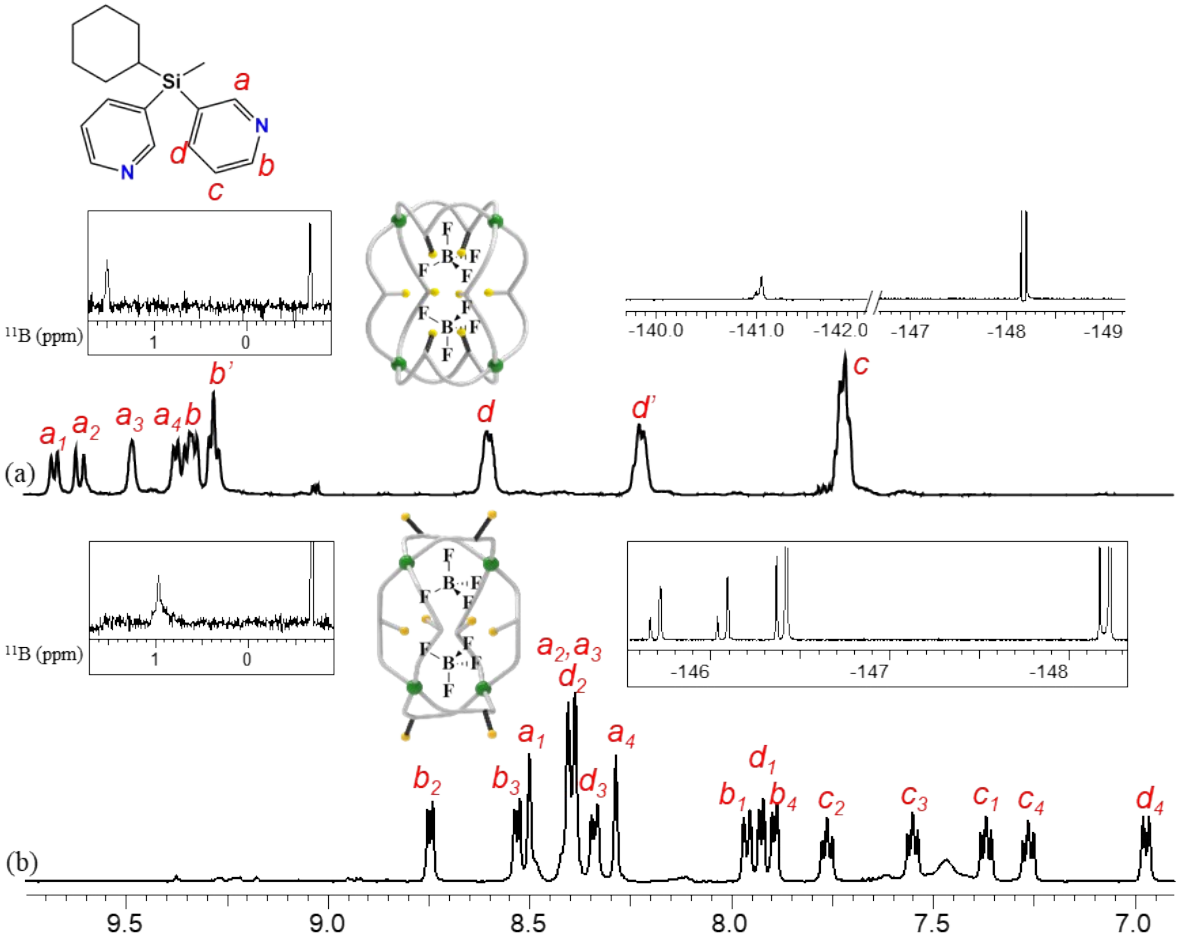

Fig. S7 ^{1}H (aromatic region), ^{11}B, and ^{19}F NMR spectra of *endo*-Me_8-$[(BF_4)_2@Pd_4L_8](BF_4)_6 \cdot 5Me_2SO$ (a, top) and *exo*-Me_4,*endo*-Me_4-$[(BF_4)_2@Pd_4L_8](BF_4)_6 \cdot 4Me_2SO$ (b, bottom) in Me_2SO-d_6, showing that the two cage isomers are stably retained in Me_2SO.

(a)

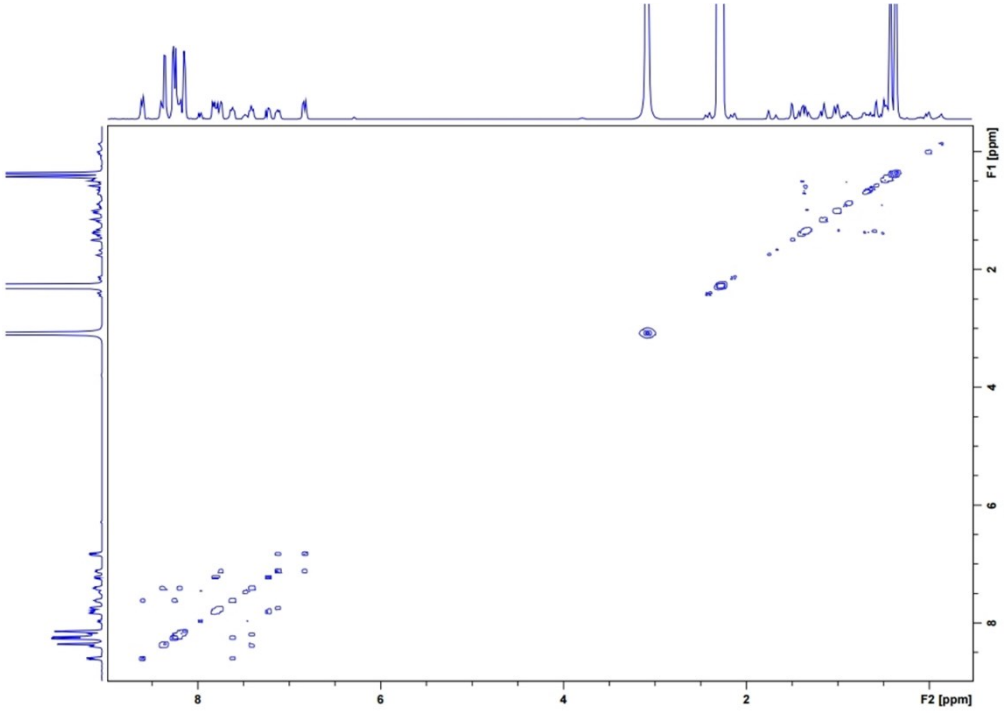
F1 [ppm]
F2 [ppm]
8
6
4
2

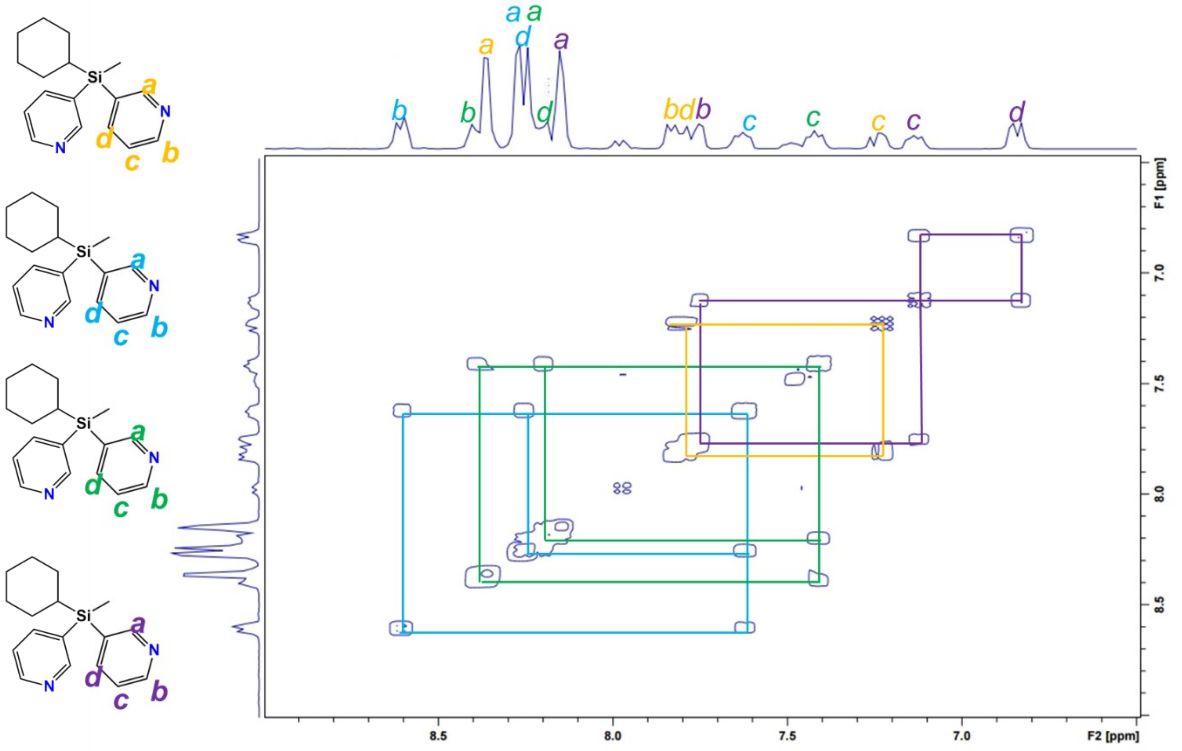
a a
a d a
b b d bdb c c c c d
Si
N
a
d
c
b
F1 [ppm]
F2 [ppm]
8.5
8.0
7.5
7.0

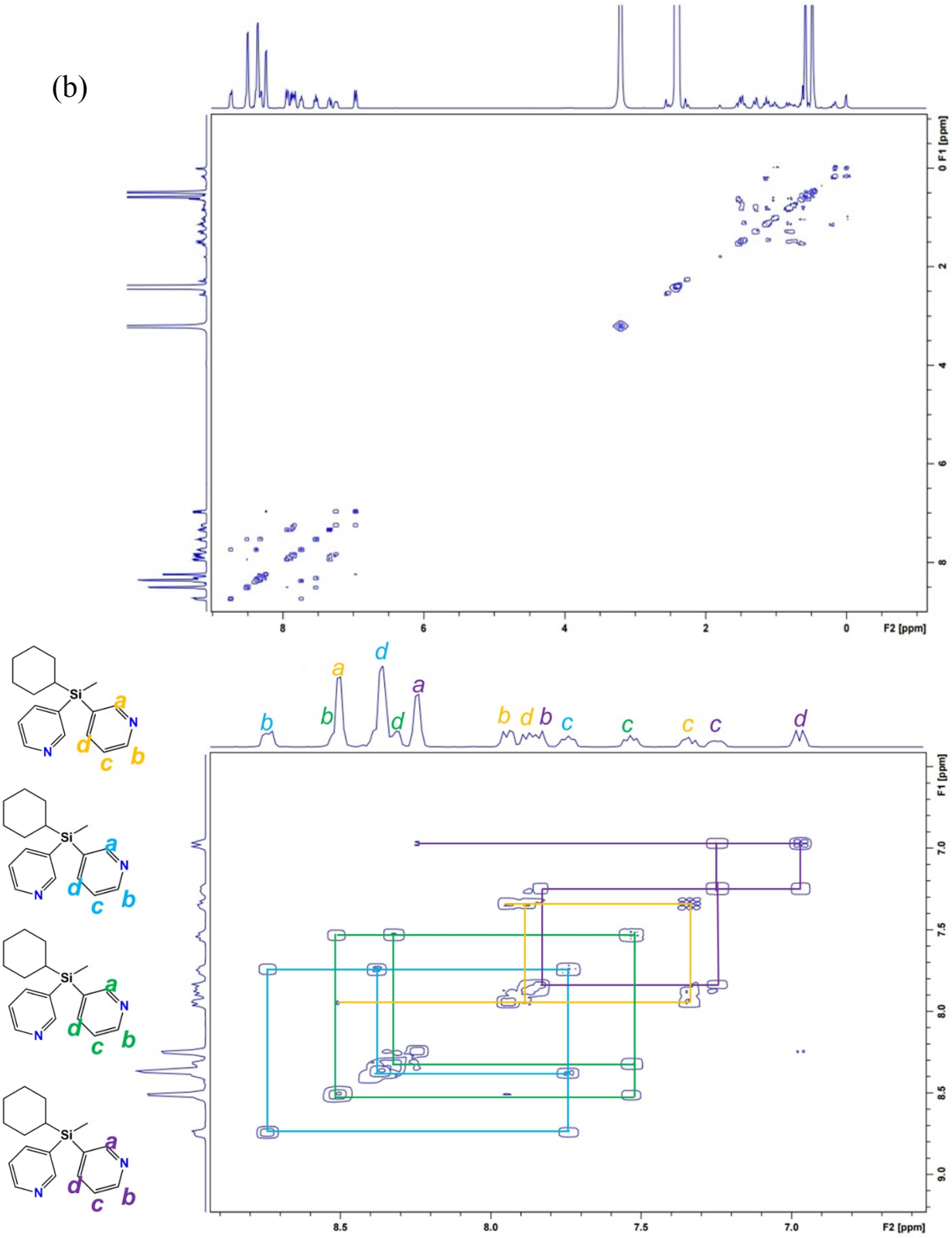

Fig. S8 COSY NMR spectra of (a) *exo*-Me_4,*endo*-Me_4-[$(BF_4)_2$@Pd_4L_8] $(BF_4)_6$·$4Me_2SO$, (b) *exo*-Me_4,endo-Me_4-[$(ClO_4)_2$@Pd_4L_8]$(ClO_4)_6$·$5Me_2SO$.

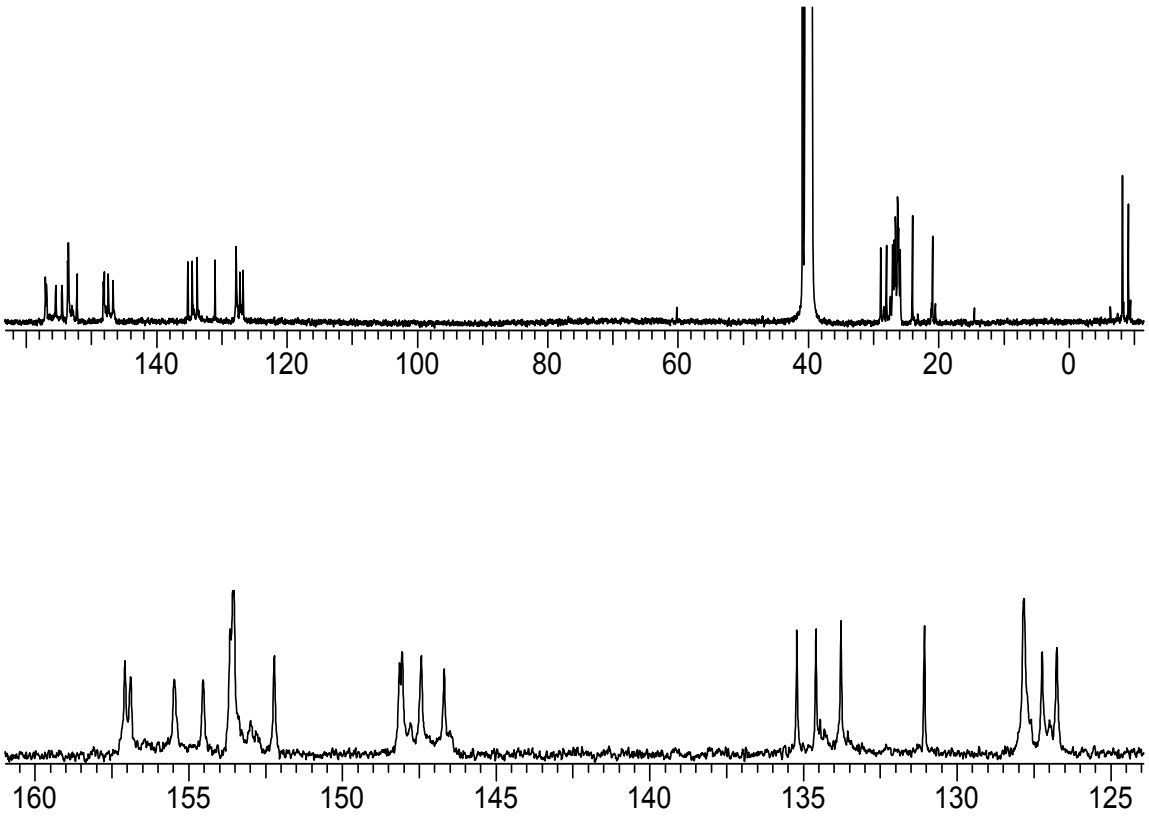

Fig. S9 ^{13}C NMR spectra of *endo*-Me_8-$[(NO_3)_2@Pd_4L_8](NO_3)_6 \cdot 5Me_2SO$.

References

1 J. W. Shin, K. Eom, D. J. Moon, *Synchrotron Radiat*., **2016**, *23*, 369–373.

2 Z. Otwinowski, W. Minor, C. W. Carter, R. M. Sweet, R. M. Methods in Enzymology, Academic Press : New York. **1997**; pp 307.

3 G. M. Sheldrick, *Acta Crystallogr. Sect. C: Struct. Chem.,* **2015**, *71*, 3–8.